IFAE 2019

Incontri di Fisica delle Alte Energie

Napoli, 8 – 10 Aprile

Misure di luminosità ad ATLAS e CMS in run pp a LHC

Comitato Scientifico:
D. Bettoni, W. Bonivento, C. Bozzi, C. Cecchi, G.G. Chiarelli, E. Coccia, P. Colangelo, F. De Fazio, A. Di Ciaccio, F. Fabbri, S. Falciano, F. Ferroni, C. Gemme, P. Lubrano, A. Masiero, L. Merola, S. Ragazzi, G. Ricciardi, B. Saitta, L. Trentadue (chair), A. Tricomi, V. Vagnoni, F. Vissani, A. Zoccoli

Comitato Organizzatore:
F. Ambrosino, G. D'Ambrosio, G. De Nardo, G. De Rosa, L. Di Fiore, A. Lauria, P. Massarotti, S. Mastroianni, M. Merola, G. Mettivier, G. Osteria, P. Paolucci, P. Santorelli, F. Tramontano, L. Valore

Sara Valentinetti on behalf of the ATLAS and CMS collaborations

Perchè la luminosità

Per ogni processo fisico con ***sezione d'urto*** $\boldsymbol{\sigma}$, il *rate di eventi R* è proporzionale alla ***luminosità istantanea*** $\mathcal{L}$ **:**

$$\boxed{\mathcal{L}} = \frac{\boxed{R}}{\sigma} = \frac{\boxed{\mu n_b f_r}}{\sigma_{inel}} = \frac{\boxed{\varepsilon\mu} n_b f_r}{\boxed{\varepsilon\sigma_{inel}}} = \frac{\boxed{\mu_{vis}} n_b f_r}{\boxed{\sigma_{vis}}}$$

μ = numero di collisioni pp inelastiche per bunch crossing

n_b = numero di coppie di bunch collidenti

f_r = frequenza di rivoluzione di LHC (11245 Hz)

σ_{inel} = sezione d'urto totale pp (~80 mb a 13 TeV)

ε = accettanza e efficienza del rivelatore

μ_{vis} = numero medio di collisioni per bunch crossing rivelato

σ_{vis} = sezione d'urto "visible" = costante di calibrazione

Misure di luminosità precise:

- $\mathcal{L}$ istantanea → monitor online LHC/trigger: performance e operatitivà (lumi levelling, monitoring del fascio…). Precisione richiesta: <3-5%

- L integrata → analisi fisiche: misure di sezione d'urto, test SM, nuova fisica (vincolare le incertezze PDF che limitano le teorie). Precisione richiesta: <1-2%

Monitor di luminosità di ATLAS per il Run 2

Luminosity measurement using a Cherenkov Integrating Detector (LUCID)

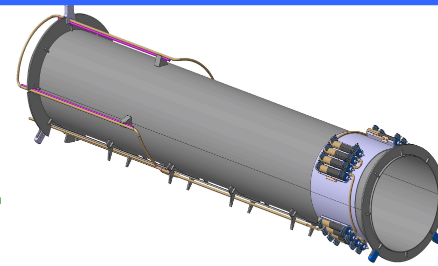

- misure **online** e **offline**
- Algoritmi event/hit counting (zero-counting, basati su statistica di Poisson)

Misure online

Beam Condition Monitor (BCM)

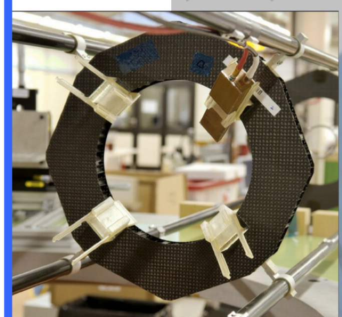

Event counting

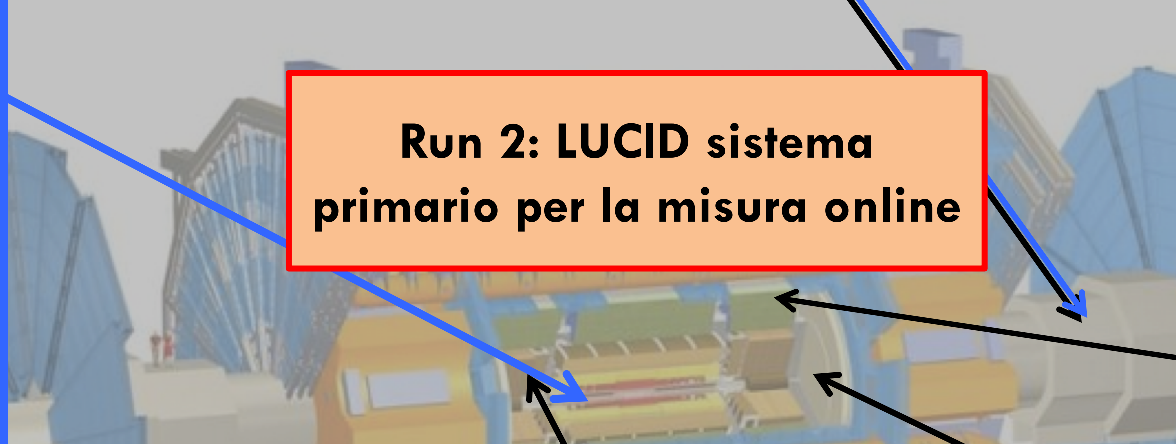

Run 2: LUCID sistema primario per la misura online

Misure offline

TimePix (TPX)

Hit counting

Hadronic Cal. (TILE)

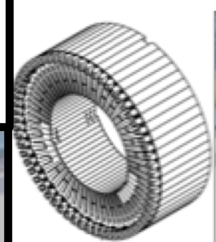

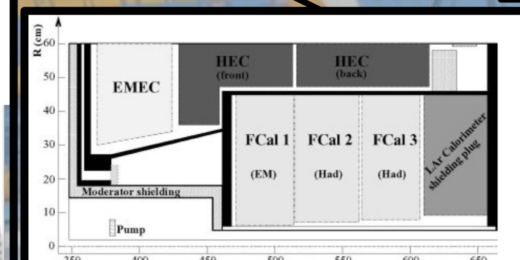

EM:
- Forward Calorimeter (FCAL)
- EndCap Calorimeter (EMEC)

+ Z counting
(controllo su L relativa)

+ Track counting
(+ Vertex counting)

Algoritmi di conteggio di flusso di particelle

Monitor di luminosità di CMS per il Run 2

Misure online

Pixel Luminosity Telescope (PLT)

Hit counting
(3-fold coinc.)

Fast Beam Condition Monitor (BCM1F)

Hit counting

Hadron Forward Calorimeter (HF)

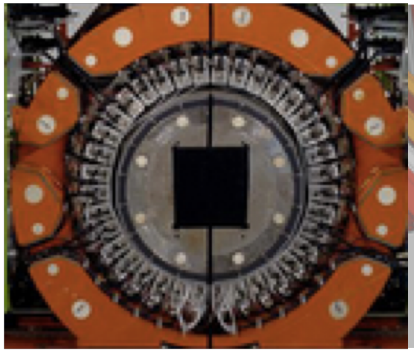

HFOC: hit counting
HFET: flusso di E_T

Misure offline

Muon Drift Tubes (DT)

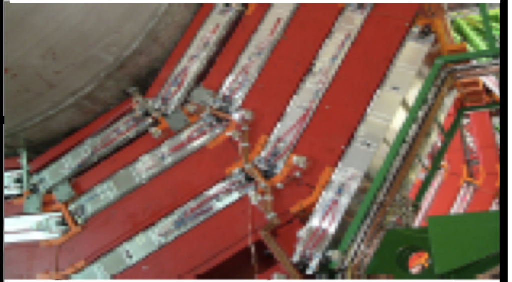

Conteggio di trigger di muoni

Silicon Pixel Detector

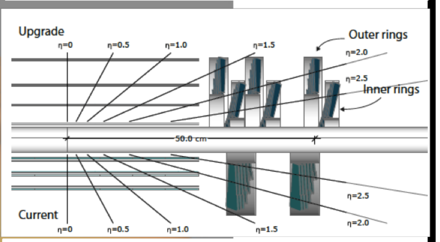

Pixel Cluster Counting (PCC)

2015/2016 basato su: PCC
2017/2018 basato su: HFET
(complementato con: PCC)

Calibrazione assoluta: vdM scan

- μ_{vis} in funzione delle separazione del fascio $\delta_{x(y)}$
- Luminosità tramite parametri del fascio

$$\mathcal{L} = \frac{n_b f_r \boxed{n_{p1} n_{p2}}}{2\pi \boxed{\Sigma_x \Sigma_y}}$$

Misure di corrente (da LHC)

Larghezza dei fasci (da fit sulla curva di scan)

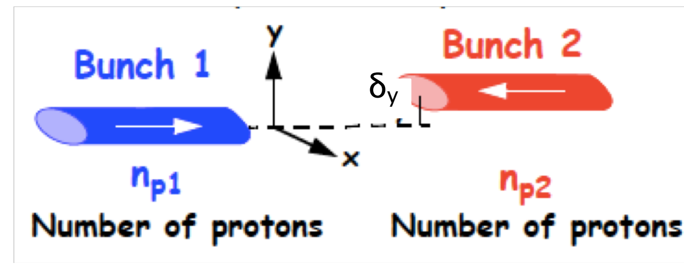

- Sezione d'urto visibile calibrata per ogni rivelatore/algoritmo

$$\boxed{\sigma_{vis}} = \frac{R}{\mathcal{L}} = \frac{\mu f_r n_b}{\mathcal{L}} = \boxed{\mu_{vis}^{peak}} \frac{2\pi\Sigma_x\Sigma_y}{n_{p1} n_{p2}}$$

- Assunzione: funzione densità di probabilità protoni fattorizzabile

$$\mathscr{L}(\delta_x, \delta_y) = f_x(\delta_x)\, f_y(\delta_y)$$

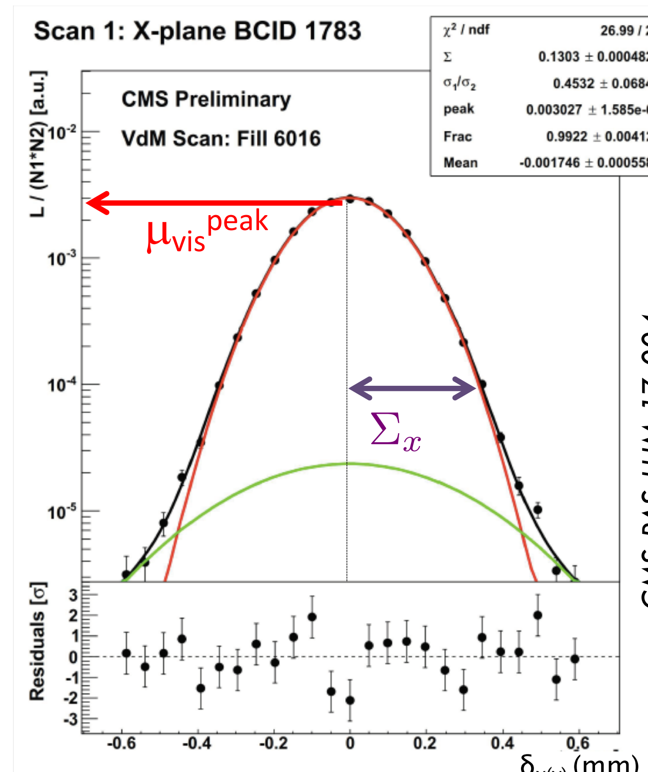

Incertezze dominanti sulla calibrazione vdM

	ATLAS	CMS	ATLAS	CMS
	2017	2017	2018 (preliminary)	2018
Non fattorizzabilità	0.2 ± 0.2%	0.8 ± 0.8%	0.3 ± 0.5%	ongoing
Riproducibilità scan per scan	± 1.2 %	± 0.9 %	±0.6%	ongoing
Calibration transfer	±1.3%	±1.5%	±1.3%	ongoing

CMS-PAS-LUM-17-004

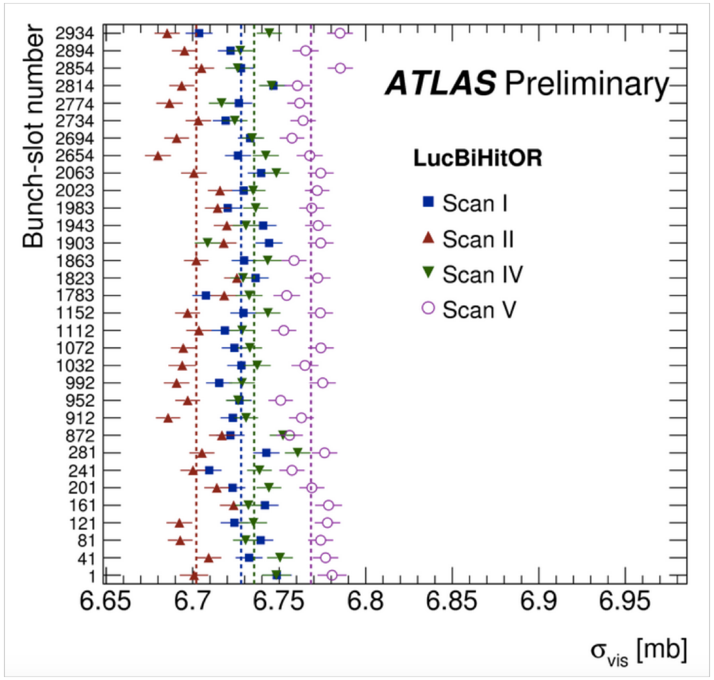

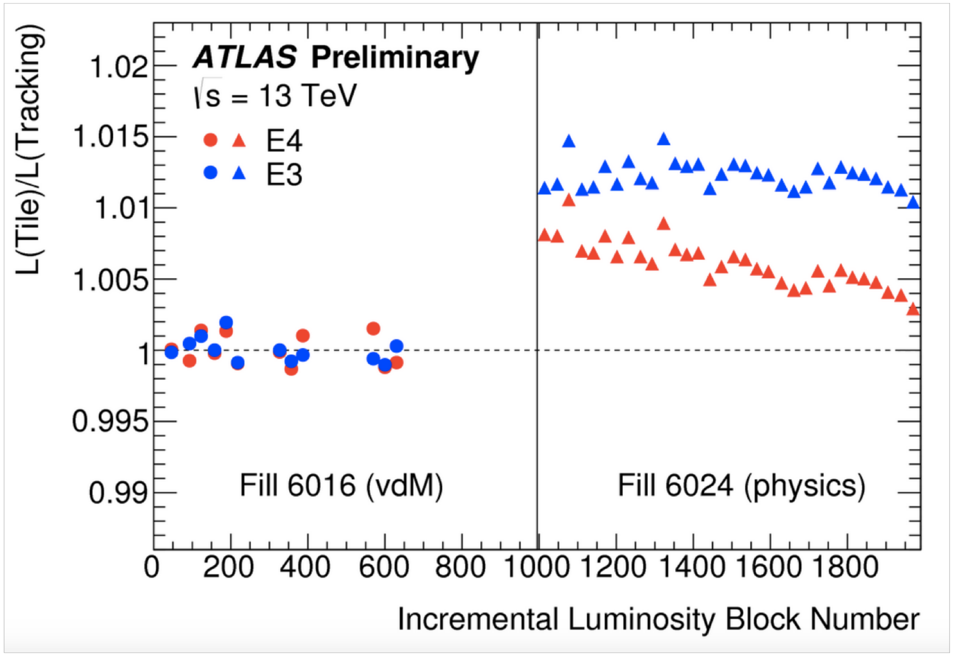

http://atlas.web.cern.ch/Atlas/GROUPS/PHYSICS/PLOTS/LUMI-2017-001/

Stabilità durante l'anno

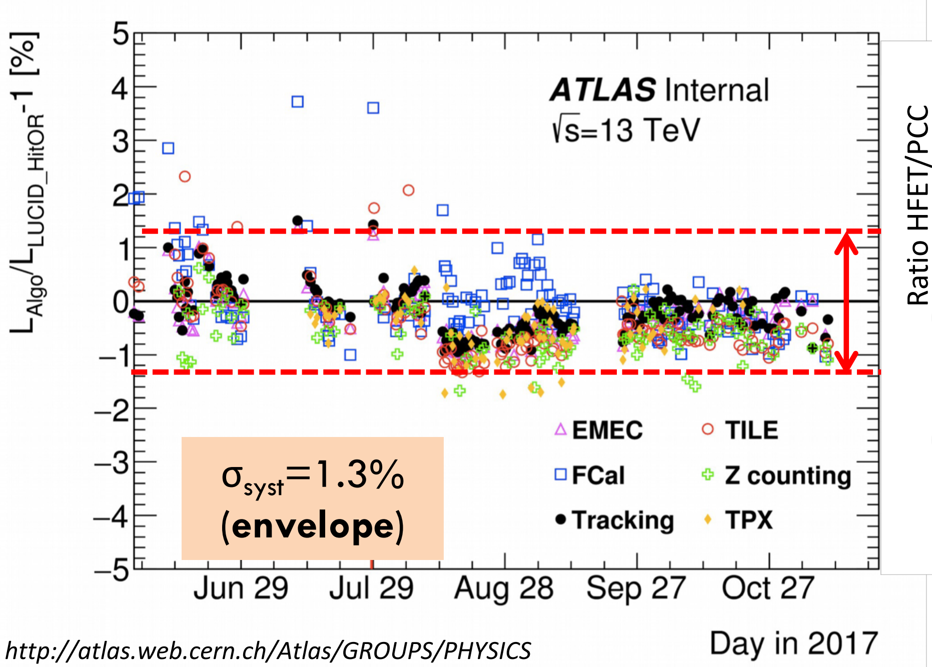

http://atlas.web.cern.ch/Atlas/GROUPS/PHYSICS/PLOTS/LUMI-2017-001/

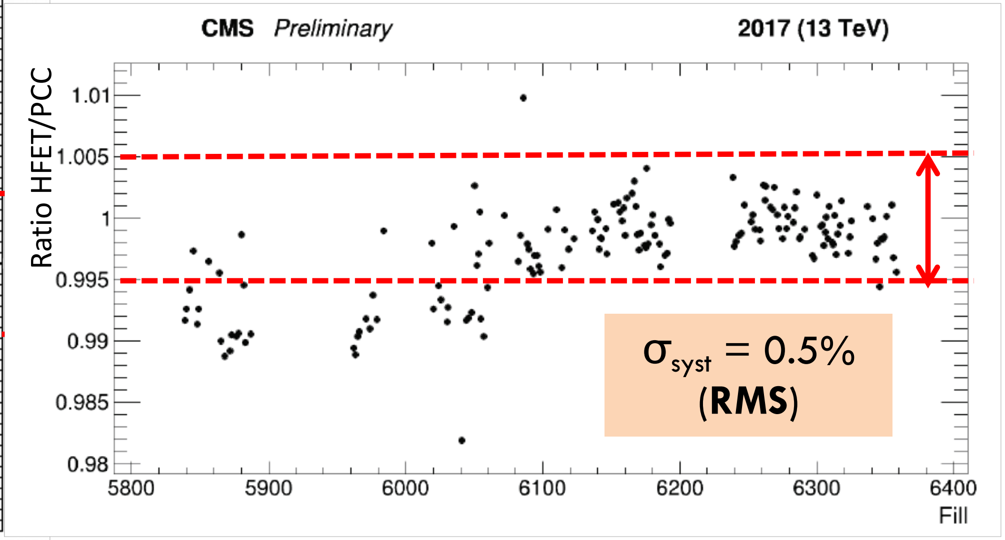

CMS-PAS-LUM-17-004

- ATLAS: confronto fra luminometri attivi durante la presa dati, incluso Z-counting (non usato per valutare l'incertezza) e Track-counting
  2017: ±1.3%; 2018: ±0.8% (preliminary)
- CMS: RMS del rapporto HFET/PCC (99.4% della luminosità nel 2017)
  2017: ±0.5%; 2018: ongoing

Incertezza sistematica totale

	ATLAS	CMS	ATLAS	CMS	ATLAS	CMS	ATLAS	CMS	ATLAS	CMS
Running period	2012 pp	2012 pp	2015 pp	2015 pp	2016 pp	2016 pp	2017 pp	2017 pp	2018 pp	2018 pp
√s [TeV]	8	8	13	13	13	13	13	13	13	13
σ_L/L [%]	1.9	2.6	2.1	2.3	2.2	2.5	2.4	2.3	2.0 Preliminary	ongoing

ATLAS: incertezza sistematica finale combinata per il Run 2:

- Incertezze non correlate: analisi vdM, stabilità a lungo termine….
- Incertezze correlate: calibration transfer…

Dataset	Int. luminosity (fb^{-1})	Rel. uncertainty
2015+2016	36.21 ± 0.77	2.1%
2017	44.31 ± 1.04	2.4%
2018	58.45 ± 1.16	2.0%
2015-2018	**139.0 ± 2.4**	**1.7%**

Preliminary

ATLAS Ref: https://twiki.cern.ch/twiki/bin/viewauth/Atlas/LuminosityForPhysics

CMS Ref: CMS-PAS-LUM-17-004/17-004/15-001/13-001

HL-LHC: ATLAS upgrade

- **Misura direttamente proporzionale alla luminosità: LUCID**
  - PMT saturati ad alto μ sostituiti con **fibre di quarzo**, readout lontano da zona radiattiva
- **Misura luminosità bunch-per-bunch: BCM'**
  - stazioni di diamanti con **3 sensori indipendenti** per luminosità, fondo e sistema di aborto del fascio
- **Timing: High Granularity Timing Detector**
  - separazione spaziale dei vertici ad alto μ tramite informazione temporale: σ_t= 30 ps.
  - **Low-Gain Avalanche Detector (LGAD)**
  - Linearità fra numero hit nel detector e numero di interazioni per bunch crossing

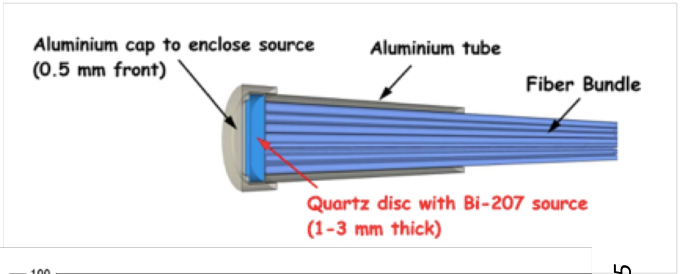

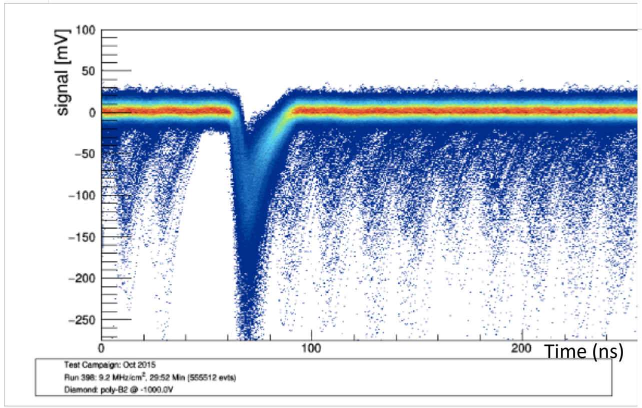

https://cds.cern.ch/record/2285585/files/ATLAS-TDR-030.pdf

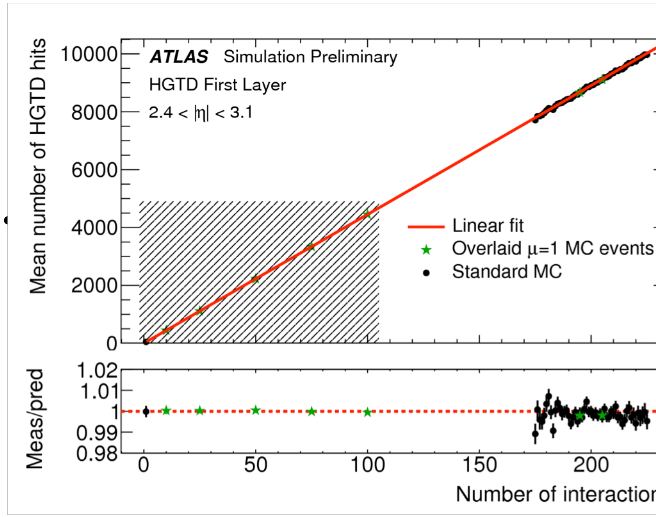

https://atlas.web.cern.ch/Atlas/GROUPS/PHYSICS/UPGRADE/CERN-LHCC-2018-023/

HL-LHC: CMS upgrade

https://indico.cern.ch/event/697164/contributions/2987411/attachments/1647549/2633730/CMSLuminosity-FCALWorkshop.pdf

Approccio multi detector (difficoltà nel dividere effetti di non linearità con solo due rivelatori)

- Inner Tracker endcap (TEPX): indipendente dal readout di CMS
- Drift Tube (DT): bassa occupanza → misure bunch per bunch
- VeloPix: Monitor di luminosità dedicato indipendente altamente resistente a danni da radiazioni
- Timing Detector: separazione spaziale dei vertici ad alto μ tramite precisa informazione temporale: σ_t= 30-50 ps/traccia.

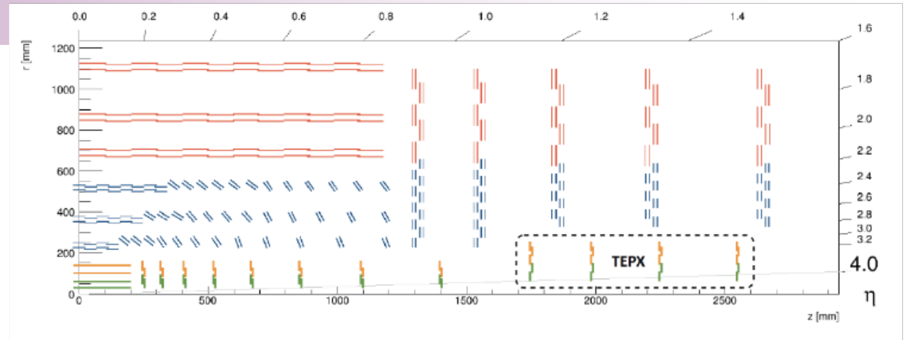

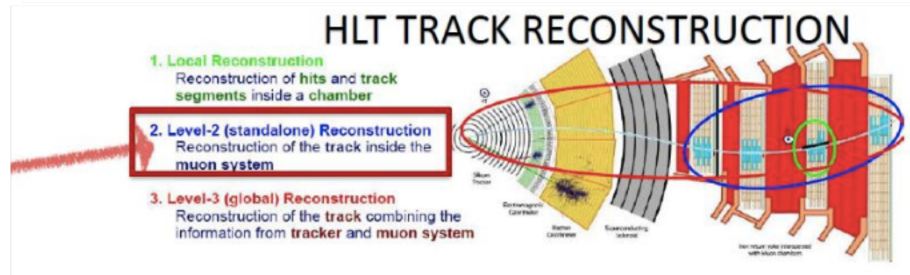

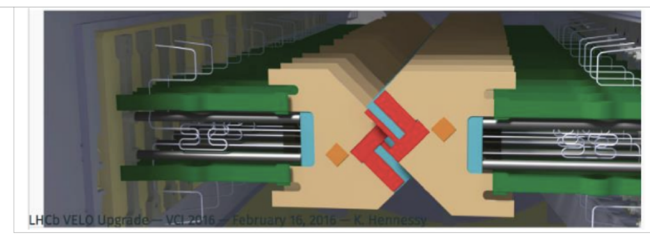

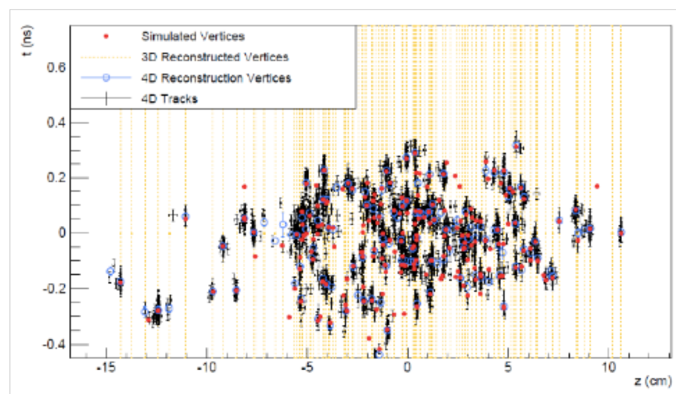

Conclusioni

- Luminosità parametro chiave per analisi di fisica ma misura complicata negli acceleratori adronici

- Ridondanza di luminometri cruciale per studio delle prestazioni e valutazione delle sistematiche: tipica incertezza sistematica totale ~2%!

- Misura della luminosità a LHC durante Run 1 e Run 2 ottenuta con precisione finale tale da permettere test di precisione sullo Standard Model e ricerche di nuova fisica.

- Prospettive future (LHC Fase II): studi in corso su upgrade dei luminometri per nuove condizioni di LHC.

Back up

Emittance scan

$$\Sigma_x^2 = 2 \langle \varepsilon_x \rangle \beta_x^*$$

At zero crossing angle

- **Brevi scan vdM** all'inizio e alla fine di ogni fill di LHC
  - Fasci separati in X e Y per 7/9 steps di 10s/punto
  - Livello di precisione inferiore rispetto vdM:
    - intervallo di scan limitato (non sensibile alle code)
    - possibli effetti di non fattorizzabilità (modo di produzione del fascio differente)
    - effetti di dinamica del fascio
  - Utili per misure di luminosità relativa

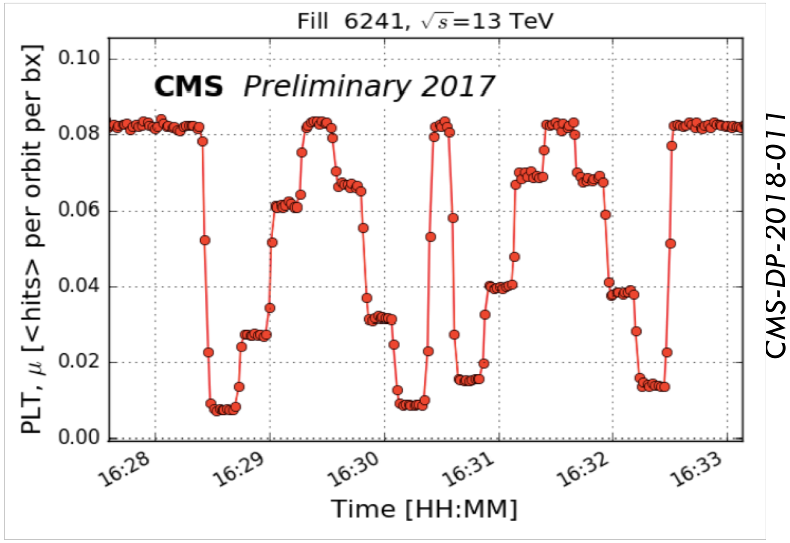

- Controllo **online effetti di linearità e stabilità**:
  - LHC: diagnostica e controllo delle prestazioni;
  - CMS (2017) e ATLAS (2018): controllo online dei luminometri.

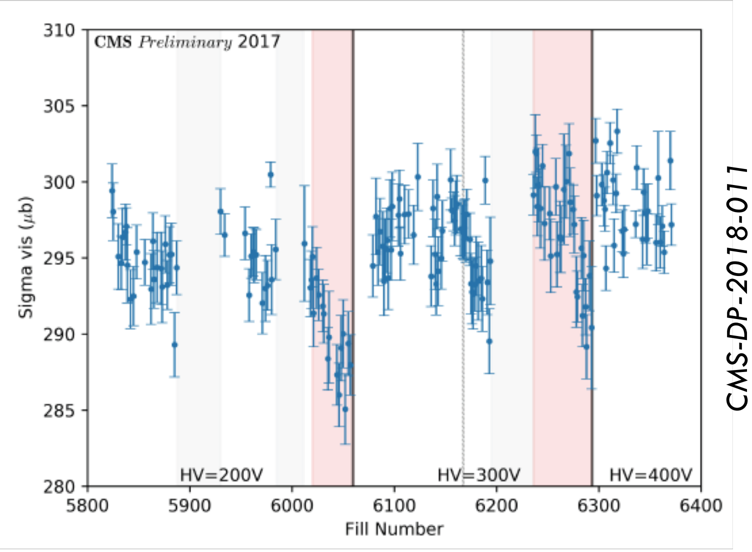

Luminosity algorithms

- Event- (or zero-) counting algorithms:
  - Based on Poisson statistics: count of events with at least one hit

$$P_{OR} = \frac{N_{OR}}{N_{orbits}} = 1 - e^{-\mu\varepsilon_{OR}} \Rightarrow \mu = -\ln(1 - \frac{N_{OR}}{N_{orbits}})$$

  - If μ too large → "zero starvation" or "saturation"
- Hit-counting algorithms: *Now: ATLAS: # LUCID hits. CMS: # pixel clusters.*
  - Count of total hits in a given BX
  - based on Poisson statistics but saturation at higher μ
- Track- (& vertex-) counting algorithms:
  - conceptually similar to hit-counting. Examples: ATLAS.
- Particle-counting algorithms (summed over all bunches)
  - Examples in ATLAS: current in hadronic-calorimeter photomultipliers or charge measurements (LUCID).

Lumi from	Detector type	Data flow	Name	Lumi Algo
ATLAS	P-CVD diamond pads	Bunch-by-bunch (bbb)	BCM	Event counting
	Quartz Cherenkov tubes	bbb	LUCID	Event counting Hit counting
	Si strip + pixel tracker: #vertices	bbb	“Vtx”	Vtx counting
	Si strip + pixel tracker: #tracks	bbb	“Trks”	Trks counting
	Fwd LAr / E.M. EndCap calo: gap currents	Bunch-averaged (ba)	FCal	Particle flux
	TILE calorimeter	ba	TILE	Particle flux
	Pixelated radiation monitor	ba	TPX	Hit counting
CMS	Pixel trk: #clusters	bbb	PCC	Hit counting
	Fwd Fe/quartz calo	bbb	HFET	E_T flow (analog)
	Fwd Fe/quartz calo.	bbb	HFOC	Hit counting
	Pixel telescope	bbb	PLT	Hit counting (3-fold coinc)
	Fast Beam Conditions Monitor	bbb	BCM1f	Trk segment counting
	Muon drift tube	ba	DT	Hit counting

ATLAS/CMS luminosity ratio

- Significant (~ 10%) ATLAS-CMS L difference across 2016

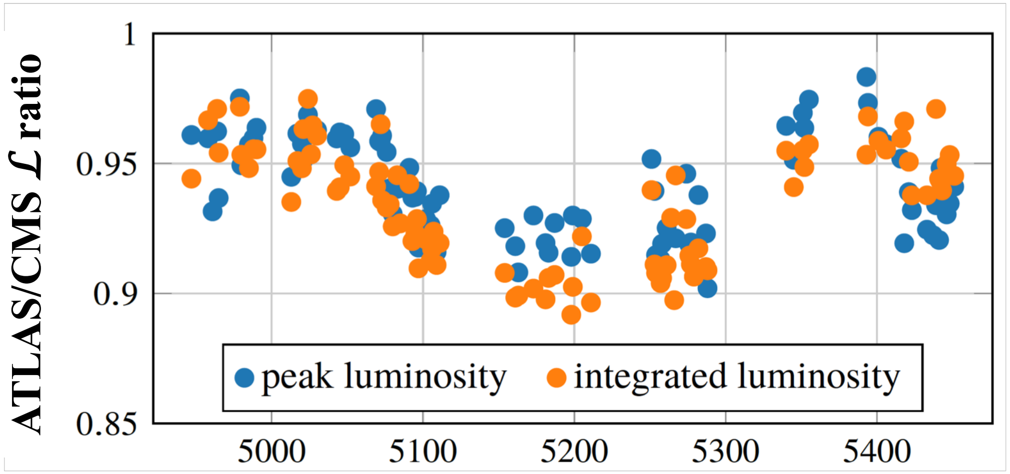

- Largest contribution: emittance$_x$ > emittance$_y$, coupled with horizontal (x) crossing in CMS vs. vertical (y) crossing in ATLAS
- Analysis complicated by residual μ- or time-dependence of reported L, that could be different in the two experiments
  - most trusted offline algorithms: track-cntg (ATLAS), pixel-cluster cntg (CMS)
  - → dedicated experiment: crossing-angle scan

Vdm Scan calibration: difficulties

Central role of beam dynamics -> two beam-beam effects:

1) beam-beam deflection: if bunches not exactly centred ➔ angular kick due to e.m repulsion;
2) dynamic β: mutual (de)focusing of the two colliding bunches;

Effect: < 0.5% PbPb, 1 - 2% for 7/8/13 TeV pp and around 4% for 5 TeV pp.

Scan curve distorted by interactions of the two beams during a scan.

Beam-beam deflection

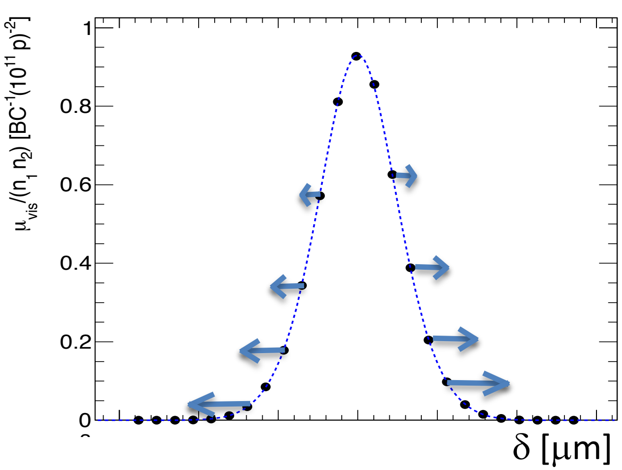

beam separation larger than nominal separation

Dynamic-β

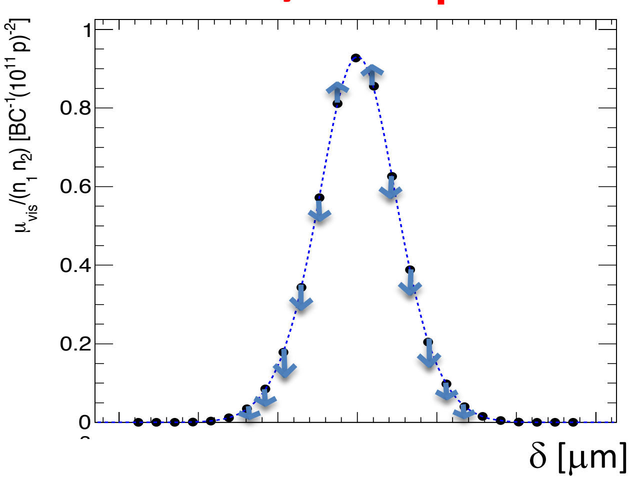

Beams focus/defocus each other by an amount that is a function of separation

Non-factorisation correction procedure

$$\mathscr{L}\left(\delta_x, \delta_y\right) = f_x\left(\delta_x\right) f_y\left(\delta_y\right) \,?$$

- Single beam profiles are parameterised by fitting the beam-separation dependence of the luminosity & of the beamspot displacement and width during a vdM scan.

  This allows to:

  → estimate the true luminosity (i.e. unbiased by non-factorisation effects)

  → estimate correction for non-factorisation, ***R***, with an associated uncertainty

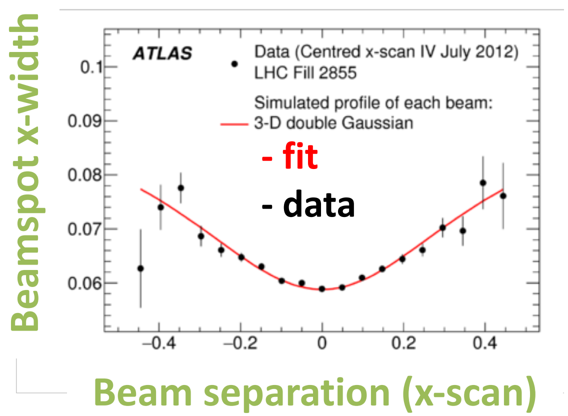

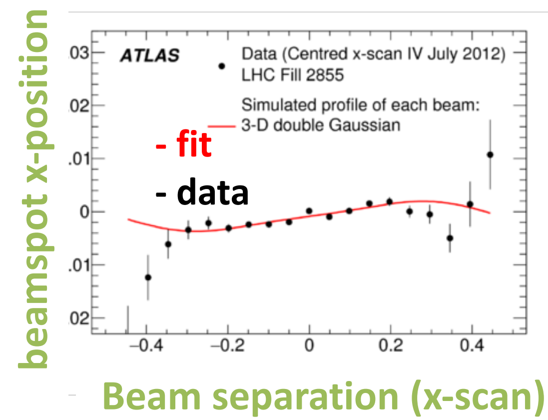

$$R = \frac{\mathscr{L} \text{ not assuming factorisation}}{\mathscr{L} \text{ assuming factorisation}}$$

- The [ATLAS/ALICE] procedure above is closely related to the “beam-beam imaging” scans [pioneered by LHCb & now established method in CMS] in which one beam is scanned transversely as a probe across the other.

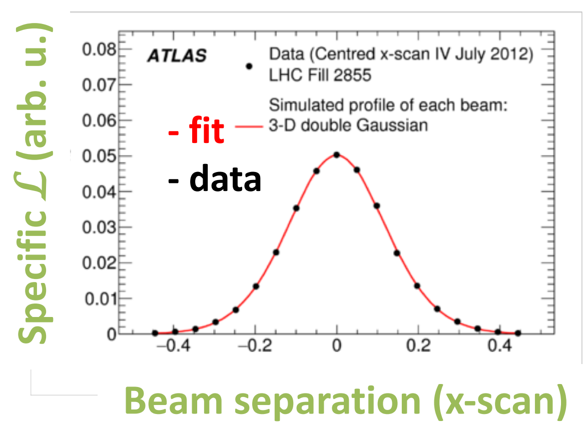

Non-factorization correction: beam-beam imaging

- Principle: use one beam (~ wire) to probe the other
  - keep witness beam (B1) stationary; scan probe beam (B2) across it in x, then in y; repeat with B1 ←→ B2
    - measure 2-d distribution of reco'd evt vertices at each step: $N_{vtx}(x, y) = \{r_{witness}(x,y) \times r_{probe}(x,y)\}\ (X)\ R_{vtx\ position}(x,y)$ (see ArXiv_1603.0356 [hep-ex])
  - extract single-beam parameters of B1 & B2 from fit to 2-d vertex distributions in the 4 scans (B1/ B2, x/y)
  - closely related to the ATLAS & ALICE luminous-region evolution method (but uses only transverse info, not L/z)
    - common key issue: vertex-position resolution $R_{vtx\ position}$
    - pros & cons of the 2 approaches to be clarified

Non-factorization correction: beam-beam imaging

Pull distribution to cumulative event-vertex distributions for 2 single-beam models:

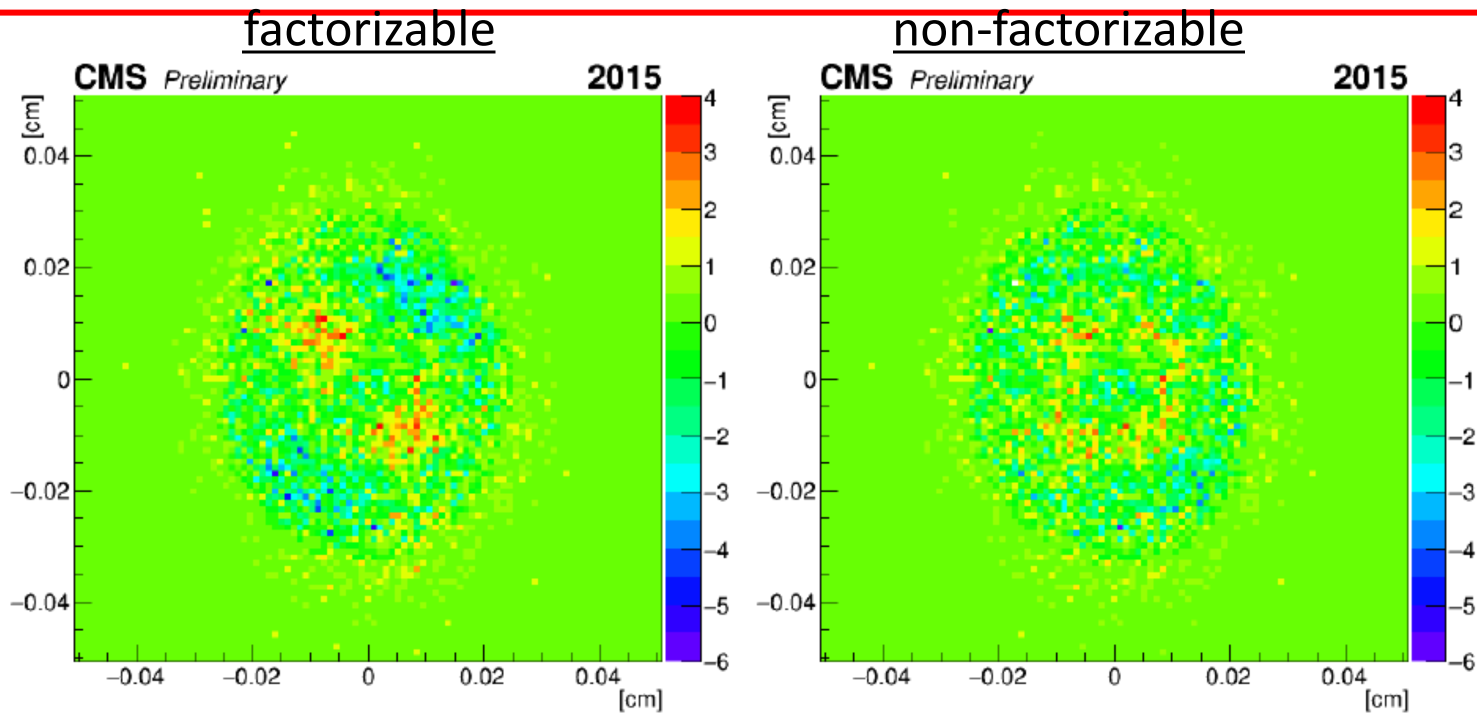

Example of pull distributions of the fitted single-beam model of the single-gaussian (factorizable, left) and double-gaussian (non-factorizable, right) type to the vertex distribution accumulated during scan Y3 of bunch pair1631.
(Caption adapted from Fig. 11 of CMS-PAS-LUM-2015-001)

Incertezze dominanti sulla calibrazione vdM

Eur. Phys. J. C 76 (2016) 653

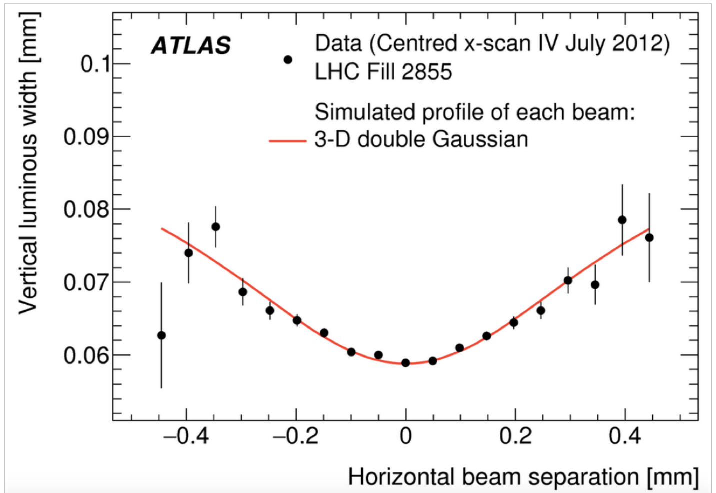

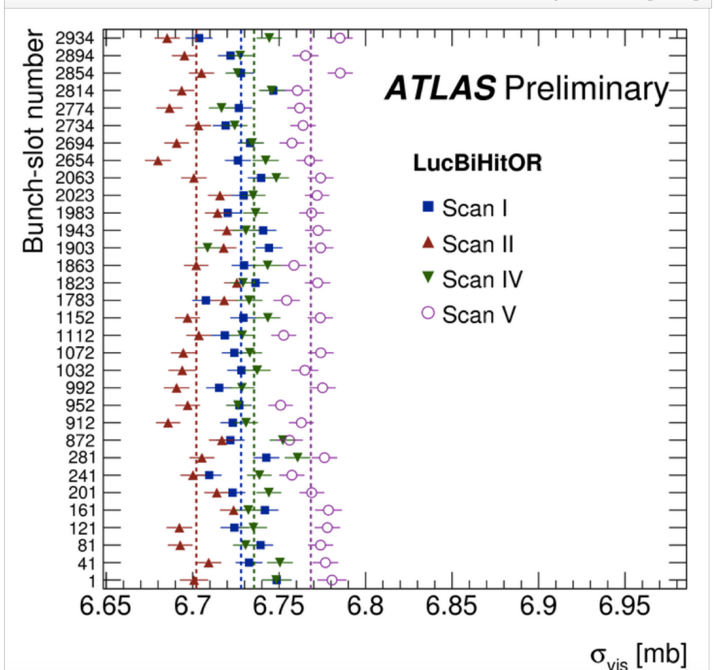

http://atlas.web.cern.ch/Atlas/GROUPS/PHYSICS/PLOTS/LUMI-2017-001/

Correzioni per effetti di non-fattorizzabilità

- dipendenza della luminosità verticale dalla separazione orizzontale e viceversa
- Correzione analisi vdM scan sotto assunzione di fattorizzabilità
  - CMS 2017: 0.8 ± 0.8%
    2018: ongoing
  - ATLAS 2017 0.2 ± 0.2%
    2018 0.3 ± 0.5%

Riproducibilità calibrazione nei diversi scans:

- CMS 2017: ± 0.9 %
  2018: ongoing
- ATLAS 2017 ±1.2%,
  2018 ±0.6%

CMS-PAS-LUM-17-004

https://twiki.cern.ch/twiki/bin/viewauth/Atlas/LuminosityForPhysics

NB: differenti strategie di valutazione delle sistematiche tra ATLAS e CMS → difficile confronto diretto

Calibration transfer: dal vdM alla fisica

Non linearità nella risposta da vdM scan (bassa $\mathcal{L}$, basso μ, pochi bunch distanziati) a fisica (alta $\mathcal{L}$, alto μ, più di 2000 bunches ogni 25 ns)

- ATLAS:
  - Correzione non linearità tramite tracciatore
    - LUCID @ $\mu = 50$
      2017: - 9.1%; 2018: - 8.9%
  - Incertezza sistematica dal confronto con calorimetri
    2017: ±1.3%; 2018: ±1.3%

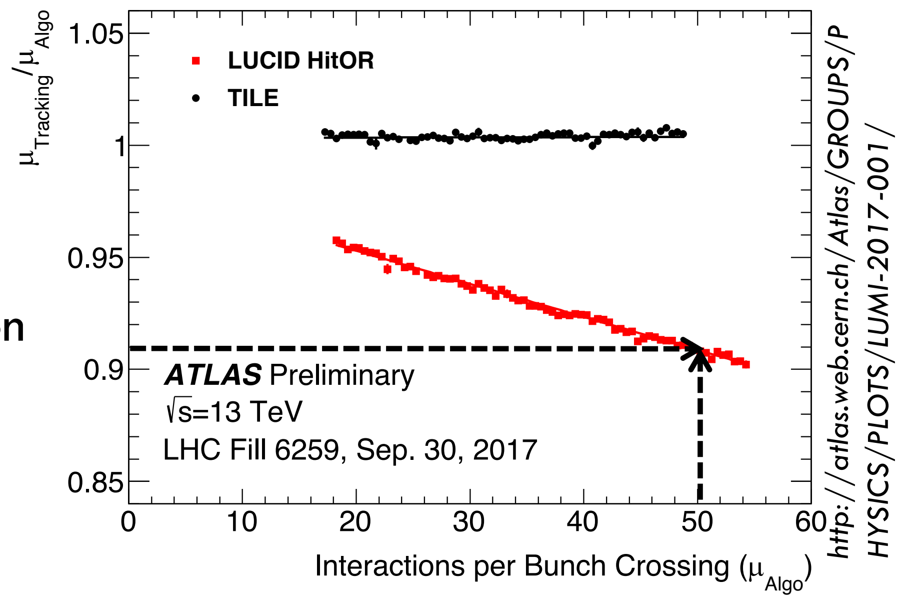

- CMS:
  - Correzione non linearità tramite analisi degli scan in emittanza
    - HFET @ $\mu = 50$ nel 2017: 1.5 %
  - Incertezza sistematica dal metodo dei residui sul confronto fra luminometri
    2017: ±1.5%; 2018: ongoing

ATLAS Ref.: https://twiki.cern.ch/twiki/bin/view/Atlas/LuminosityForPhysics
CMS Ref.: *CMS-PAS-LUM-17-004*

ATLAS: Non factorization evidence

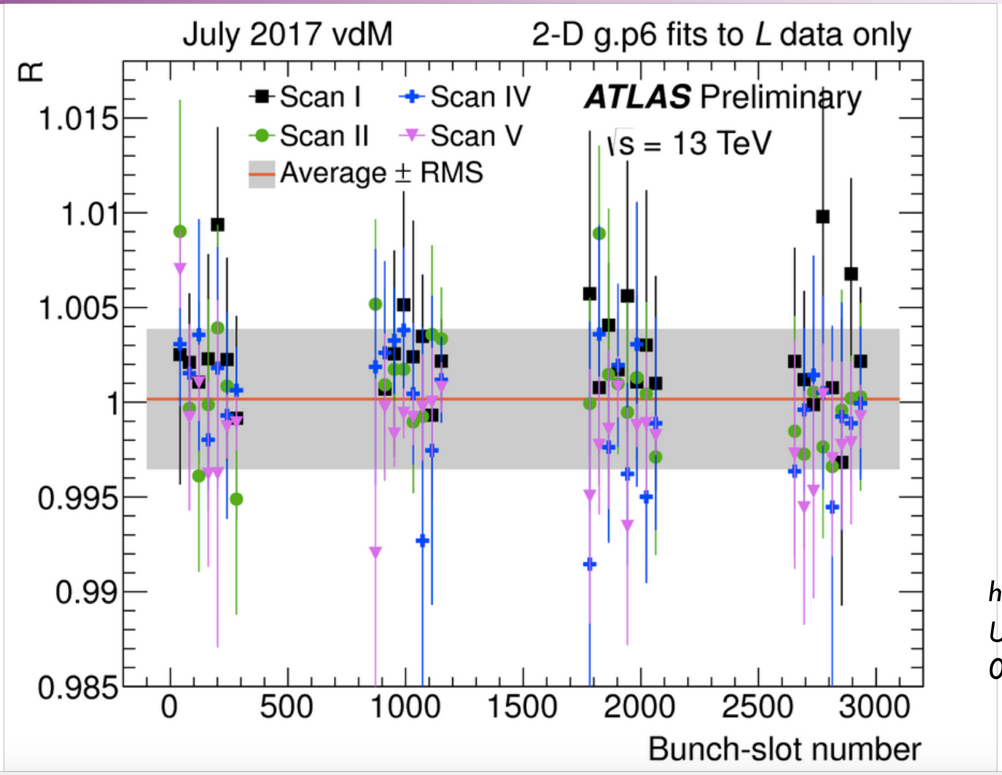

http://atlas.web.cern.ch/Atlas/GROUPS/PHYSICS/PLOTS/LUMI-2017-001/

Figure 3a:

Non-factorization correction factor R ($\sigma_{vis}^{corr}=\sigma_{vis}/R$) for several colliding-bunch pairs and scan sets (I-V), extracted from fits to the beam-separation dependence, during van der Meer (vdM) scans, of only the luminosity L. The beam-separation dependence of the luminosity is modeled by a two-dimensional (2-D) Gaussian function multiplied by a sixth-order polynomial (g.p6). The error bars are statistical only. The horizontal red lines represent the weighted average over all colliding-bunch pairs and scan sets, with the shaded bands indicating the RMS spread of the individual R values associated with each colliding-bunch pair.

ATLAS: Calibration transfer

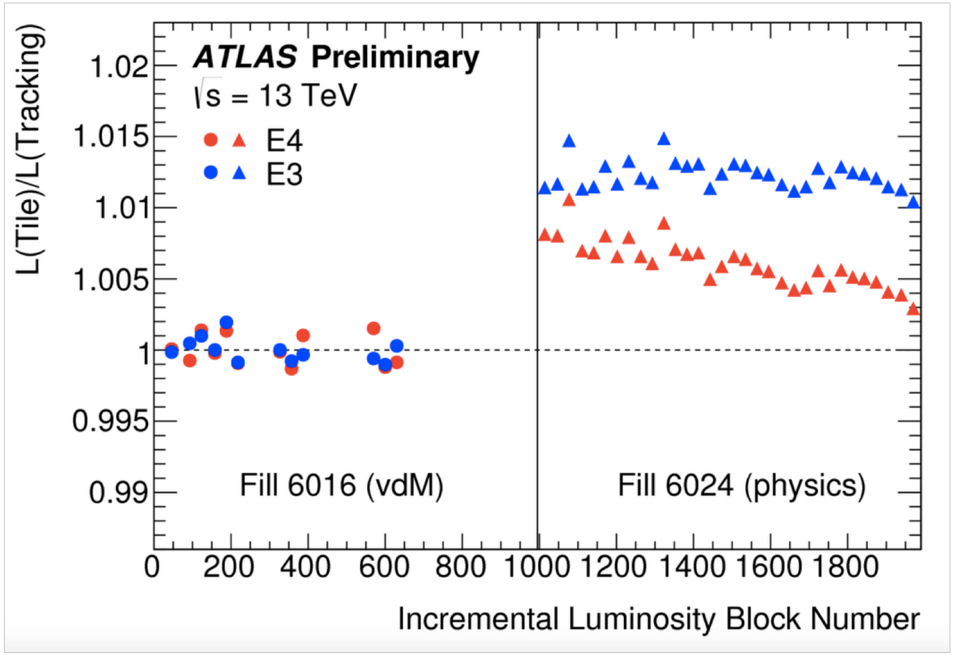

http://atlas.web.cern.ch/Atlas/GROUPS/PHYSICS/PLOTS/LUMI-2017-001/

Figure 8:

Ratio of the luminosity measured by the E3 and E4 Tile scintillators (averaged over the A and C sides of ATLAS) to that from track counting, in the 2017 vdM fill and a closely following high-luminosity physics fill. The ratios are normalised to unity in the vdM fill. Each point corresponds to the average over 30 luminosity blocks (approximately 30 minutes). The luminosity block numbers in the two runs have been offset so the physics fill begins at 1000.

CMS: Non factorization evidence

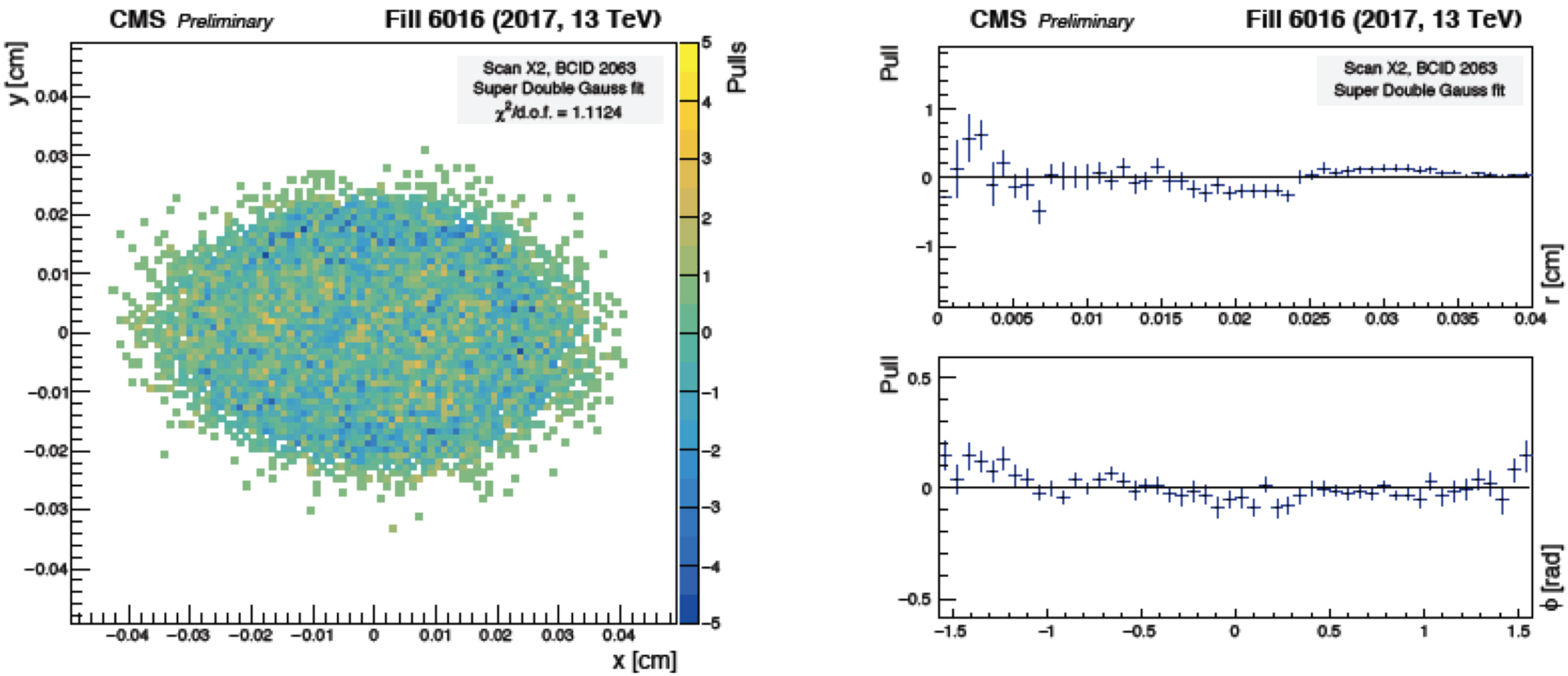

CMS-PAS-LUM-17-004

Figure 6: Pull distributions using the Super Double Gaussian fit model. The pull is defined as the difference between the number of measured vertices and the number of vertices predicted by the fit, divided by the statistical uncertainty of the measurement. These plots show the results from the scan constraining beam 1 in x. Left: 2-D pull distribution as a function of x and y position. Right: 1-D projections of the 2-D pull distribution, in slices of constant radius (top) and constant azimuthal angle (bottom).

CMS: summary of 2017 uncertainties

Table 4: Summary of the systematic uncertainties entering the CMS luminosity measurement for $\sqrt{s} = 13$ TeV pp collisions. When applicable, the percentage correction is shown.

	Systematic	Correction (%)	Uncertainty (%)
Normalization	Length scale	-0.9	0.3
	Orbit drift	—	0.2
	x-y correlations	+0.8	0.8
	Beam-beam deflection	+1.6	0.4
	Dynamic-β^*	—	0.5
	Beam current calibration	—	0.3
	Ghosts and satellites	—	0.1
	Scan to scan variation	—	0.9
	Bunch to bunch variation	—	0.1
	Cross-detector consistency	0.4–0.6	0.6
Integration	Afterglow (HF)	—	$0.2 \oplus 0.3$
	Cross-detector stability	—	0.5
	Linearity	—	1.5
	CMS deadtime	—	0.5
	Total		2.3

CMS-PAS-LUM-17-004

ATLAS reference luminometer: LUCID-2

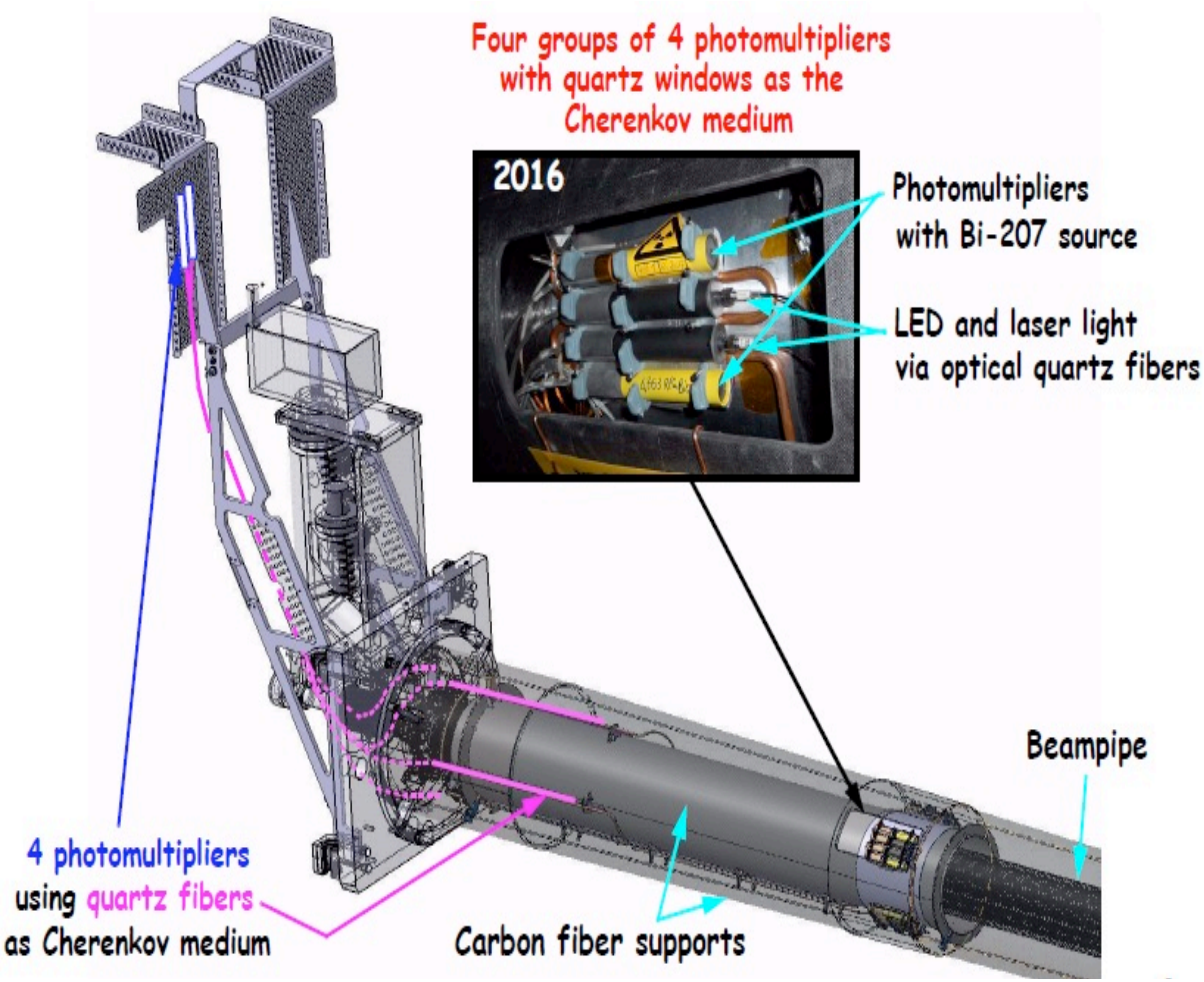

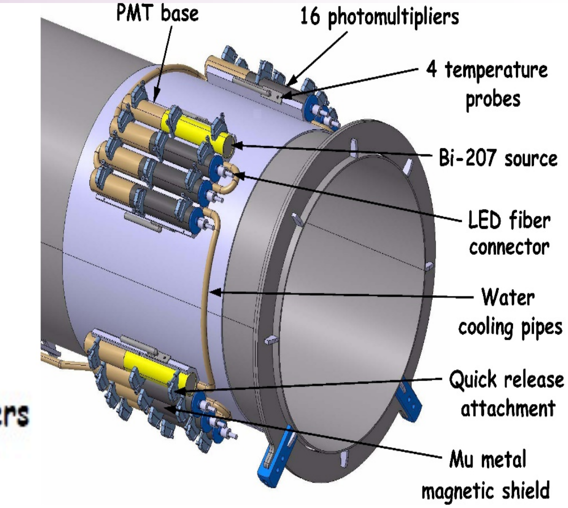

17 meters from IP – 13 cm from beam-line

ATLAS Luminosity performance summary

Year	c.m. energy (TeV)	Mu max	L_max (10^{33} $cm^{-2}s^{-1}$)	L_int (fb^{-1})	NBCID	Dt (ns)	Tot Sys Unc. (%)	vdM Sys. Unc. (%)	Reference Detector (online & offline)
2010	7	5	0.2	0.047	348	150	3.5	3.4	LUCID-I
2011	7	20	3.6	5.5	1331	50	1.8	1.5	BCM
2012	8	40	7.7	22.7	1368	50	1.9	1.2	BCM
2015	13	28	5	4.2	2232	25	2.1	1.7	LUCID-2
2016	13	45	14	38.5	2208	25	2.2	1.2	LUCID-2
2017	13	80	20	40	2544	25	2.4	1.5	LUCID-2

Year	c.m. energy (TeV)	β* (m)	L_Inst ($10^{30}c^{-2}s^{-1}$)	L_Int (μb^{-1})	Tot Sys Unc. (%)	vdM Sys. Unc.(%)	Reference detector
2011	7	90	$5*10^{-3}$	80	2.3	1.5	BCM
2012	8	90	$5*10^{-2}$	500	1.5	1.2	BCM
2012	8	1000	$0.8*10^{-3}$	22	1.4	1.2	LUCID

CMS: PLT

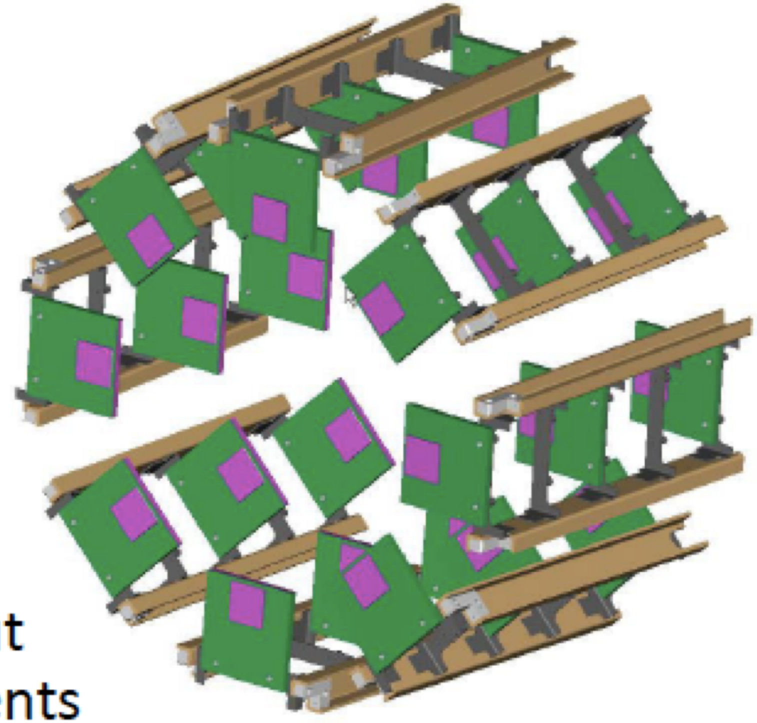

- Uses same pixel sensors and readout chips as phase-0 pixel detector
- 48 silicon sensor planes arranged in 16 “telescopes” (8 on either side of CMS) outside the pixel endcap ($|\eta|\sim 4.2$)
- Use special “fast-or” readout mode of chip to look for events where all three planes in a telescope register a hit (“threefold coincidence”) to measure luminosity
- Provide online bunch-by-bunch measurements to LHC and CMS with a statistical precision of 1% every 1.5s to allow for fast feedback (e.g., for beam optimizations)

CMS: BCM1F

- 24 sensors located on face of PLT/BCM1F carriage with fast readout (6.25 ns) to distinguish luminosity from machine background
- 2015-2016 all sensors were diamond, but severe problems with efficiency loss in 2016
- In EYETS sensors were replaced and upgraded to a mix of polycrystalline diamond, single crystal diamond, and silicon

EYETS 16/17

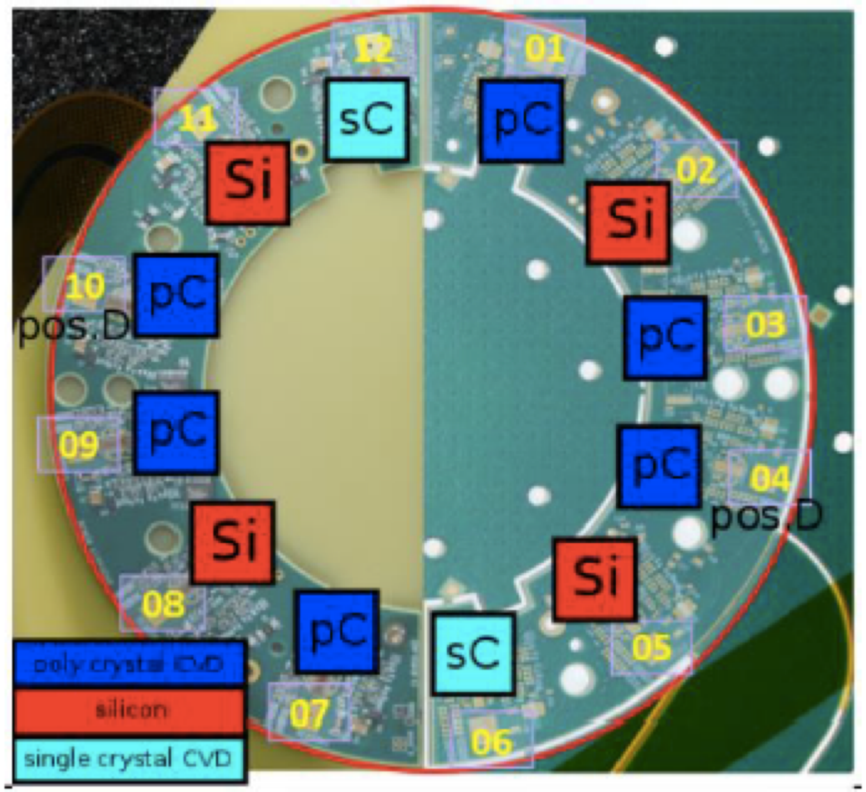

CMS: PCC

- Pixel cluster counting uses the raw rates of pixel clusters in the main CMS pixel detector
  - Primary offline measurement in 2015 and 2016 (Phase 0 pixel detector)
  - Limited by CMS DAQ and trigger for online practicality
- Two major corrections necessary:
  - "Type 1" affect the next BX after a colliding BX for signal spillover
  - "Type 2" affect several BXes after for material activation

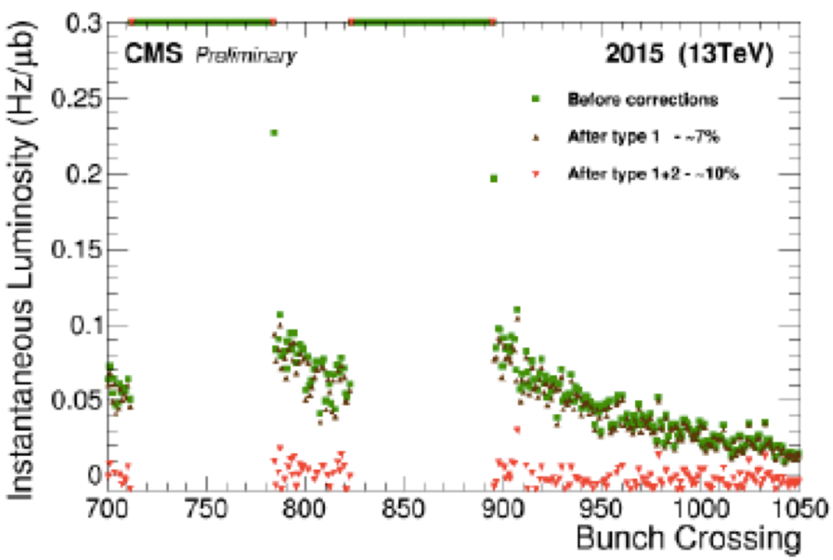

CMS-PAS-LUM-15-001

CMS: HF

- Uses existing HF calorimeter with dedicated readout for luminosity information
- Two algorithms used:
  - HFOC: uses raw occupancy rate in HF (fraction of towers with hit energy above noise threshold). Standard in 2015-16 but some nonlinearities at higher pileup.
  - HFET: uses sum of E_T deposited in all HF towers. Commissioned during 2016 and is now the primary algorithm for 2017-2018 running.

Upgrade per HL-LHC

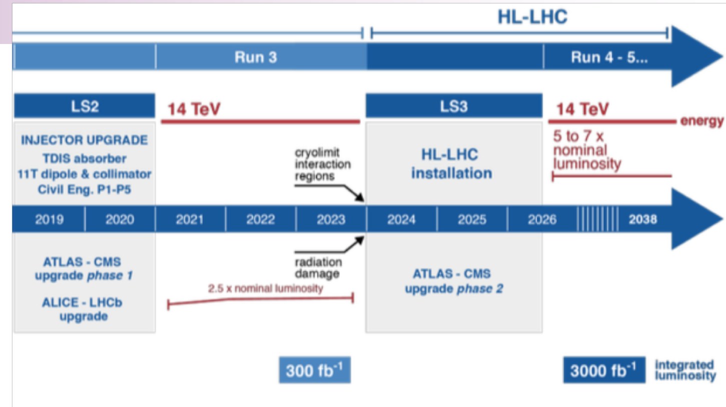

Prestazioni attese HL-LHC:

- Energia nel centro di massa: $\sqrt{s}$ = 14 TeV
- L istantanea = 5.0×10^{34} cm^{-2} s^{-1}
- L integrata = 3000 fb^{-1}
- Numero medio interazioni per bunch crossing: $\langle\mu\rangle$=200

Difficoltà tecniche:

- Alto flusso di particelle, alto trigger rate
  - ➢ nuovo sistema di trigger
- Alta occupanza rivelatori
  - ➢ Limitazioni readout
  - ➢ Complessità di ricostruzione evento
- Aumento della fluenza vicino alla beam pipe fino a 10^{16} n_{eq} /cm^{-2}
  - ➢ danni da radiazione
  - ➢ attivazione dei materiali

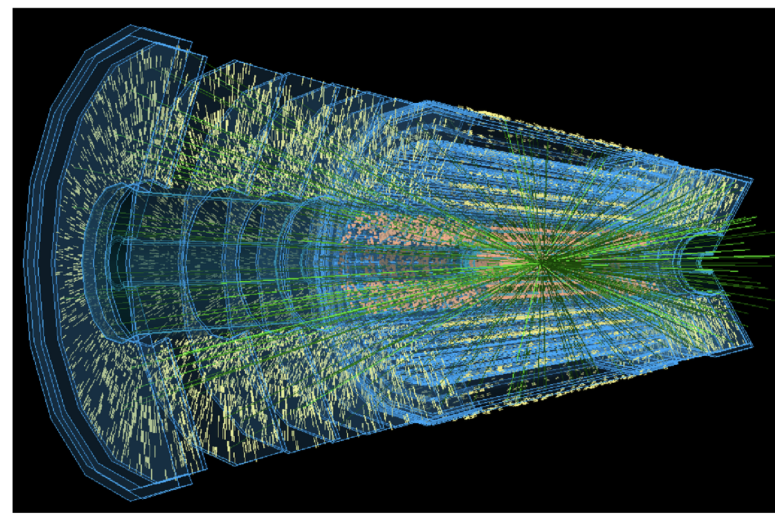

https://twiki.cern.ch/twiki/bin/view/AtlasPublic/UpgradeEventDisplays

HL-LHC: ATLAS

ATLAS $\mathcal{L}$-upgrade: a possible future LUCID fiber detector

- With μ-values going up to 140-200 the present type of quartz photomultiplier detector will saturate (hits in every BXs).
- Present idea for LUCID-3: fiber detector with a Bi-207 source at the end of the fiber bundles that provides Cherenkov light for calibration

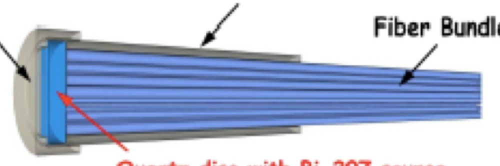

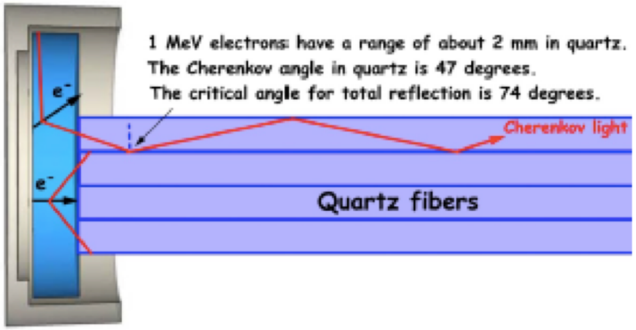

- Prototyping started
  - 2.45 m long PUV800 quartz fiber bundle with 35 fibers; each end epoxied in ferrules and polished
  - One fiber end was connected to a Hamamatsu R760 photomultiplier. At the other end, 50 ml of a Bi-207 solution was applied directly to the fibers & let to dry.

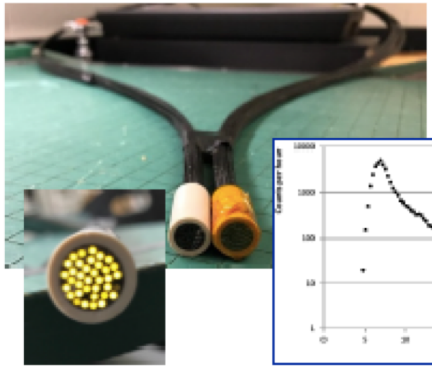

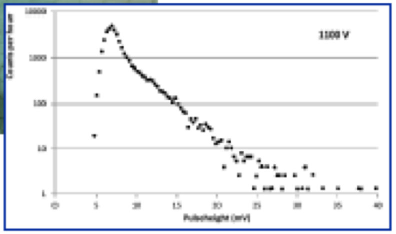

W. Kozanecki *Slide 16* *FCAL Collaboration meeting, Kraków, 10 May 2018*

HL-LHC: ATLAS

ATLAS $\mathcal{L}$-upgrade: (one of the applications of) the HGTD [High-Granularity Timing Detector]

- **Original (& primary) motivation**
  - High vertex density & degraded z_0-resolution at high η → ambiguous track-to-vertex association
  - Spatially overlapping vertices can be resolved in the time dimension using accurate vertex timing measurements
- **HGTD in a nushell**
  - two endcap disks at $z = \pm$ 3.5 m
  - Active area: 120 mm < R < 640 mm $\Rightarrow 2.4 < |\eta| < 4.0$
  - Si-based Low-Gain Avalanche Detector (LGAD) technology $\Rightarrow \sigma_t$ = 30 ps/track over the lifetime of HL-LHC
  - 2 Si layers per disk
  - RQ < 10% occupancy @ μ = 200 $\Rightarrow$ 1.3 mm x 1.3 mm pixels

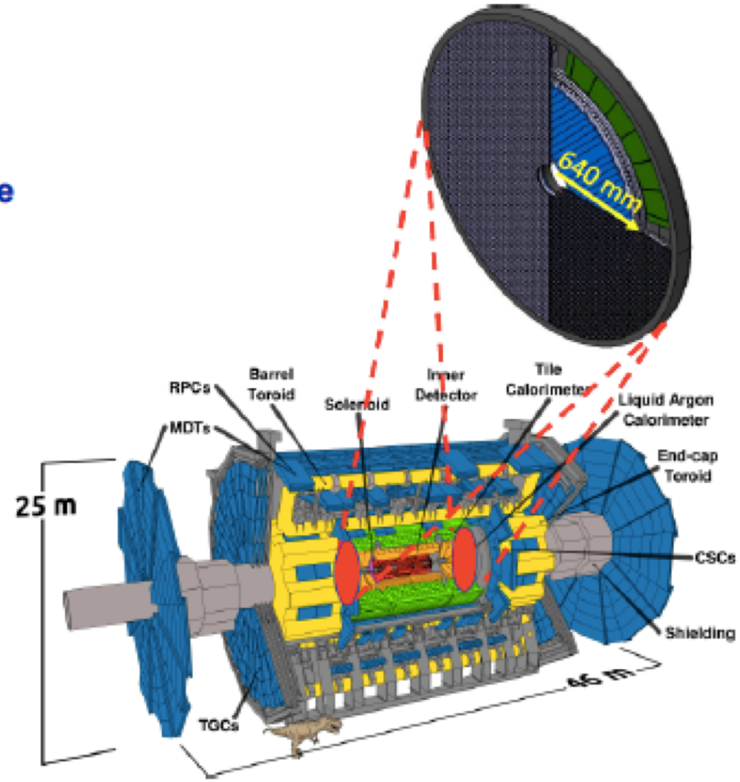

W. Kozanecki *Slide 17* *FCAL Collaboration meeting, Kraków, 10 May 2018*

HL-LHC: ATLAS from CMS experience

HGTD $\mathcal{L}$ measurement: Pixel Cluster Counting (PCC)

- **Use pads 2.8 <|η| < 3.1**
  - **high granularity → no saturation**
    - **10% occupancy easily handled by Poisson formalism**
  - **good statistical power over full μ range**

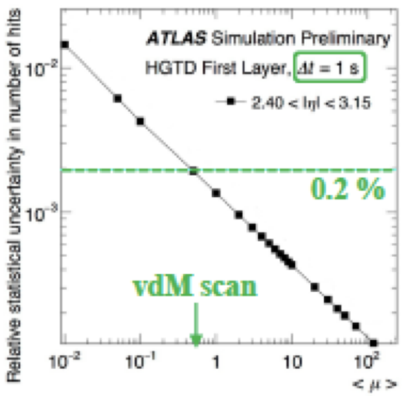

- **Deadtime-less, bbb readout**
  - **Hit count per ASIC (2 cm x 2 cm area) at 40 MHz (every BX on every turn) for**
    - **central time window, and, separately, for**
    - **sideband(s) for afterglow subtraction**
      - **take advantage of good time resolution**

- **Excellent linearity…**

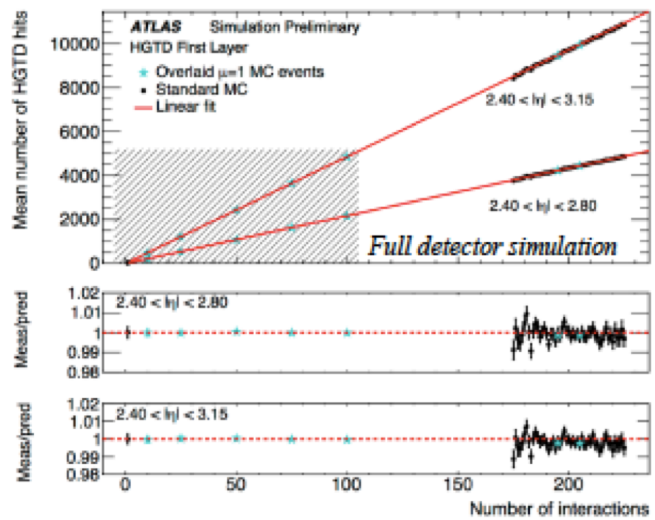

… in simulation!

- **This effort would greatly benefit from acquiring real-life experience with PCC-based $\mathcal{L}$ determination using the forward-pixel disks in the present ATLAS detector**

W. Kozanecki *Slide 18* *FCAL Collaboration meeting, Kraków, 10 May 2018*

CMS: special read out of Inner Tracker

Luminosity measurement with HGTD

- Exploit correlation between the number of hits in the detector and the number of interactions per bunch crossing
- The number of multi-hits in a single pixel is expected to be negligible (especially in the outer part of the detector 2.4<|η|<3.1)
- The after-glow can be suppressed comparing the number of hits during a bunch crossing with the number of hits after a bunch crossing

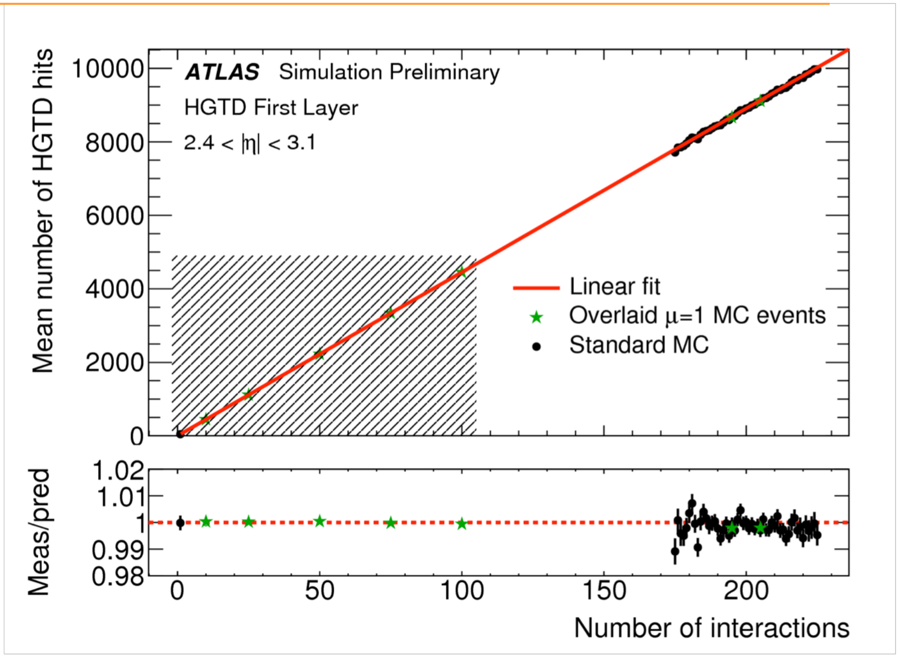

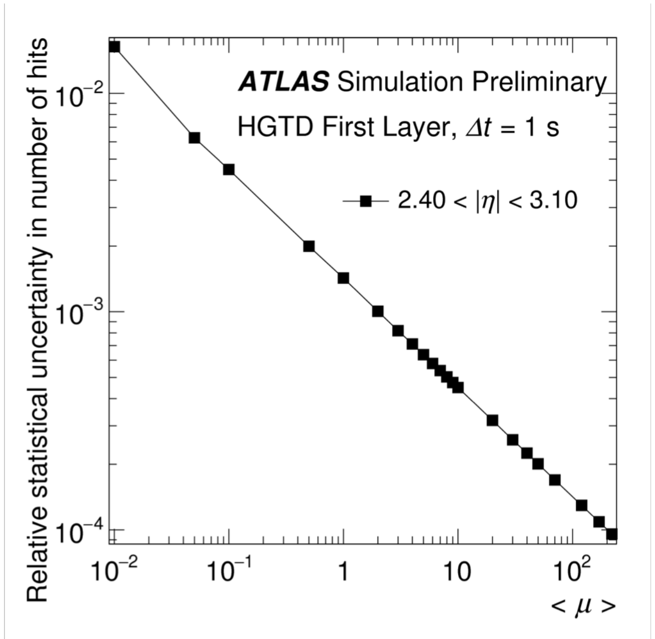

- HGTD will allow unbiased high-statistics per-BCID luminosity measurements integrating all the hits in a period of 1s.
- A statistical precision of 0.14% for a run with an average number of simultaneous p-p interactions <μ>=1 and down to 0.01% for a run with< μ>=200 is possible.
- Better precision could also be achieved through a longer averaging time.

HL-LHC: ATLAS BCM’

Reasons:

- handle on the background activity in the tracker, with the aim of aborting LHC beams when danger levels approached.
- online bunch-by-bunch luminosity measurement at 1% precision.

Run 2 problematics:

- Current BCM provided by two systems:
  - fast BCM: both as a bunch-by-bunch abort and luminosity device.
  - Beam Loss Monitoring (BLM): diamond sensor integrating the charge over a minimum of 40μs.
- two functionalities provided by a resistive splitting of the very fast signal -> non-optimal performance on both tasks:
  - For luminosity: the speed results in degraded S/N, so signal amplitude variations induce efficiency drift.
  - For abort beam: luminosity requires single MIP sensitivity but this limits the level of the abort threshold settings, making them hard to justify, especially with only a few circulating bunches in the machine ,when the slow BLM’s fail to show any activity

HL-LHC: ATLAS BCM’

- stations with 3 fully separate devices (pCVD diamond pad sensors): luminosity, fast and slow abort. The 1 cm2 diamond sensors of luminosity and abort devices are divided into7 pads of decreasing sizes from 32 to 1 mm2to effectively cover the foreseen dynamic range. The time-of-flight flagging of beam induced background used in the current BCM is kept. Background-induced showers originating upstream provoke signals early by2z/c≈12.5 ns (for the 1.9 m “golden” z location) in 4 stations on the upstream side with respect to the signal

https://cds.cern.ch/record/2285585/files/ATLAS-TDR-030.pdf

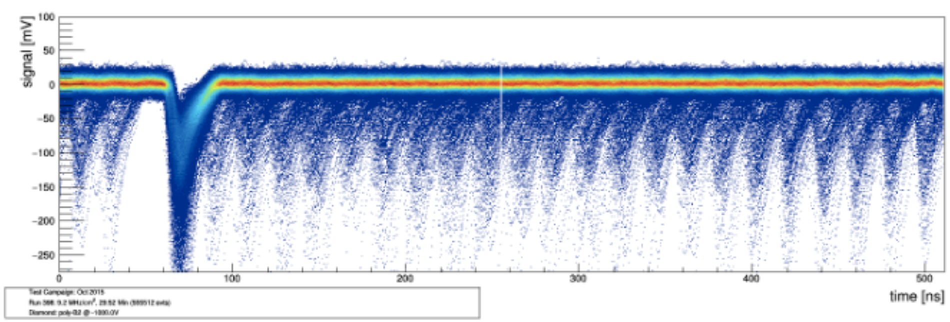

Figure 12.6: Persistency plot of the PSI beam at 9.2 MHz/cm^2 with the BCM′ amplifier prototype. The approximately 20 ns time structure is clearly resolved. The absence of the bunch before the triggered one is due to trigger veto.

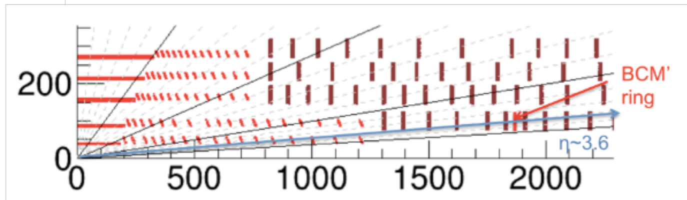

HL-LHC: CMS

Inner Tracker Endcap

- The larger tracker for HL-LHC will take up the space currently occupied by PLT & BCM1F
- However the endcap disks (TEPX) are in a perfect position to do a similar luminosity measurement

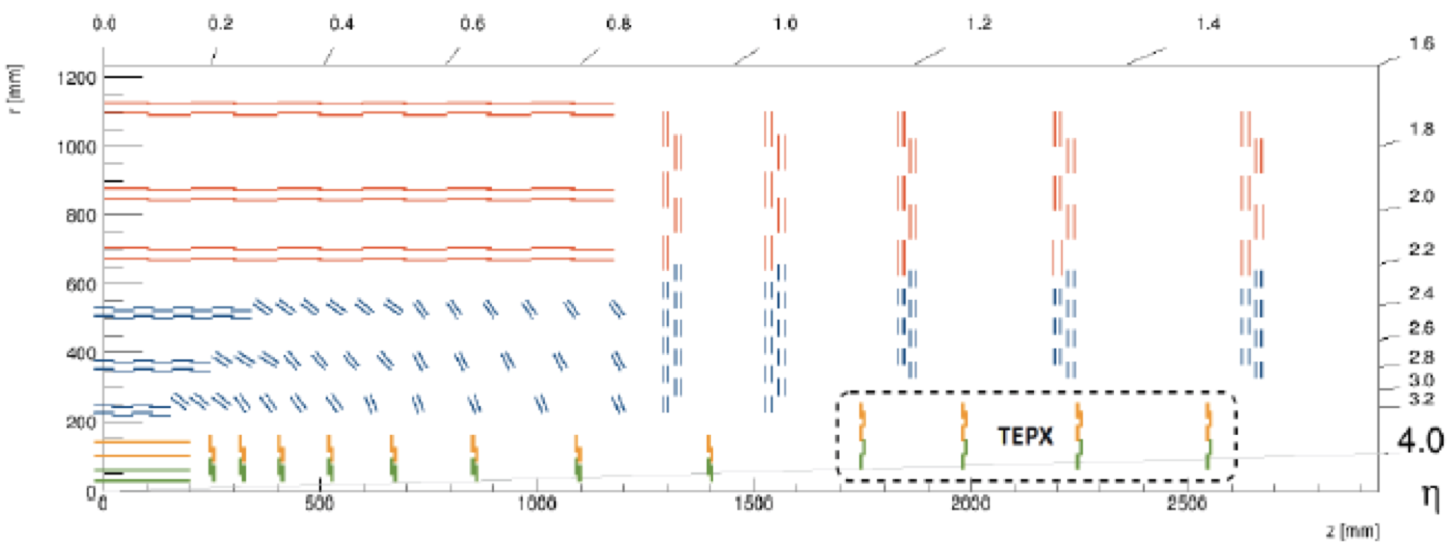

https://indico.cern.ch/event/697164/contributions/2987411/attachments/1647549/2633730/CMSLuminosity-FCALWorkshop.pdf

HL-LHC: CMS

Standalone Lumi Detector

- It is also desirable to have a completely independent lumi system
- Promising approach using VeloPix: very radiation-hard pixel chip being developed for LHCb VELO upgrade
- Could squeeze a single layer in the space outside the tracker

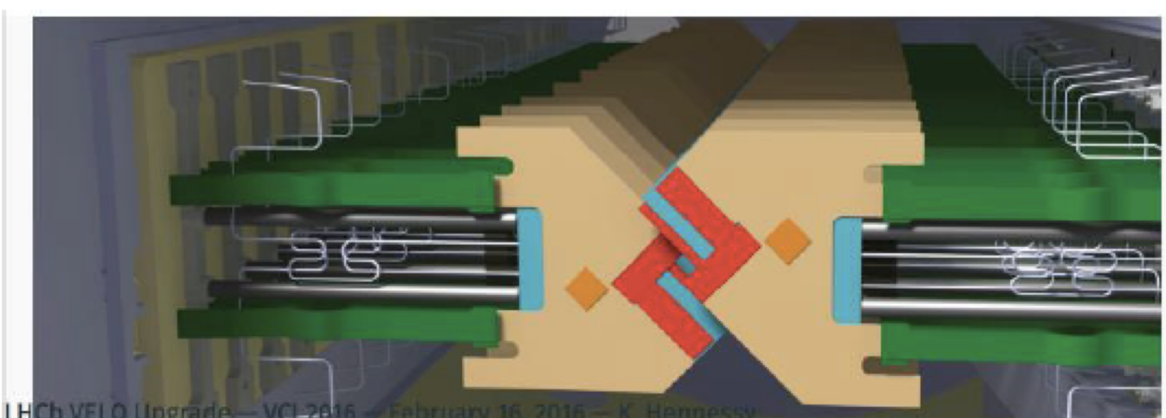

HL-LHC: CMS

DT Lumi

- As currently, it looks like the most advantageous approach to using the muon chambers is to take advantage of tracks reconstructed at trigger level
- Should be possible in principle to make bunch-by-bunch measurements available (may even be possible, at least as a prototype, in Run3 after LS2)
- Overall occupancy should remain quite low even at HL-LHC levels

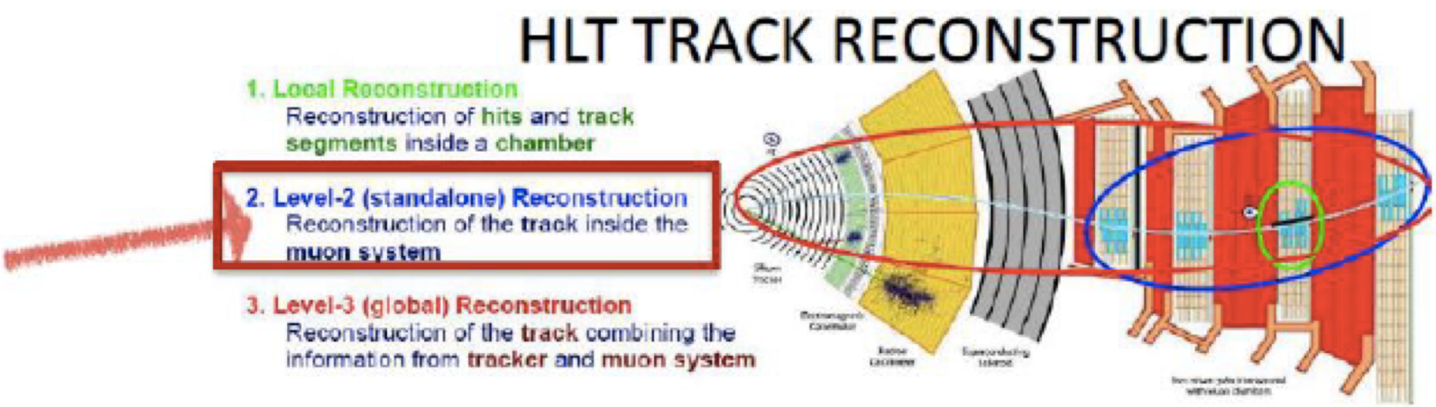

HL-LHC: CMS

Lumi with Timing Detectors

- Timing layer outside tracker to provide high-precision time measurements to improve PF reconstruction
- High time resolution (30-50ps) makes this promising as a luminosity measurement also
- Still just an idea at this point…will need much more development

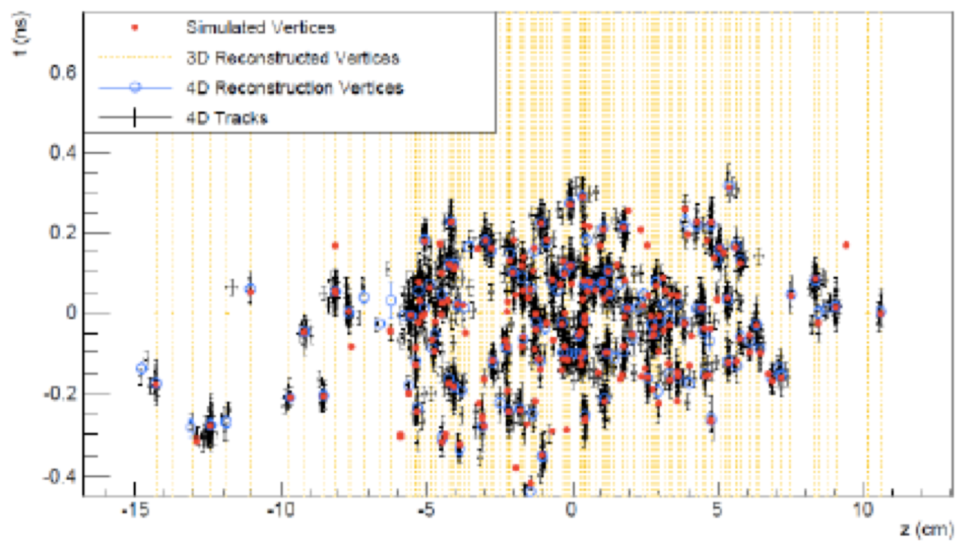

ATLAS Z-counting

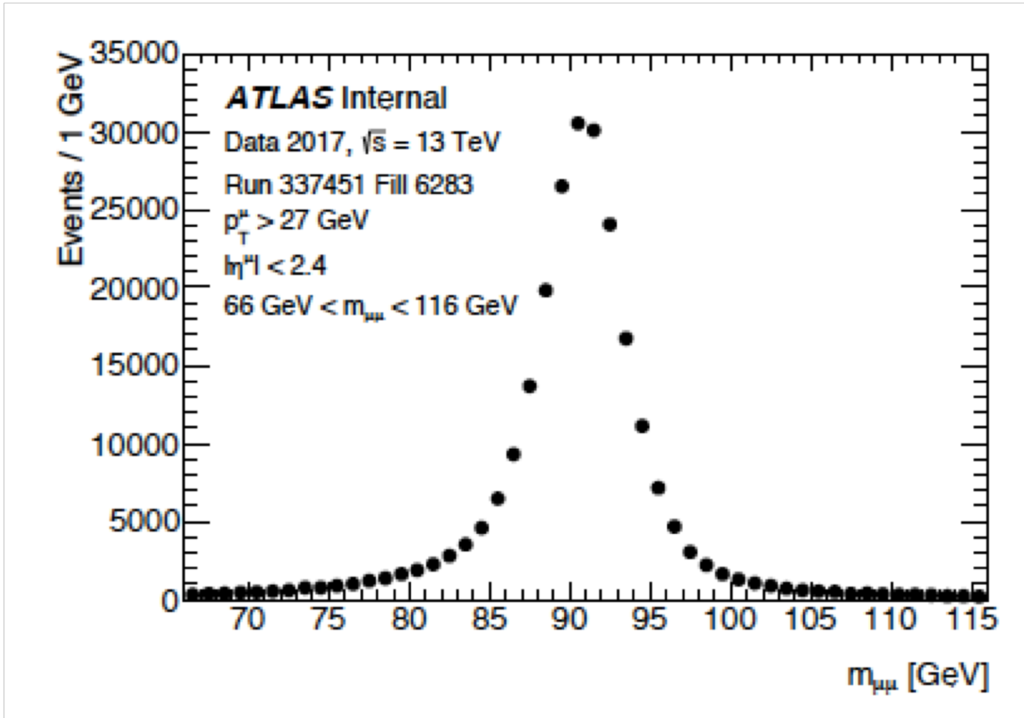

ATL-COM-DAPR-2018-011

The invariant mass distribution of the muon pairs of the 240,000 Z ->mumu boson events selecting two muons with pT> 27 GeV, pseudorapidity < 2.4 and 66 < m(mumu) < 116 GeV. The statistical errors are smaller than the symbol size.

ATLAS Z-counting

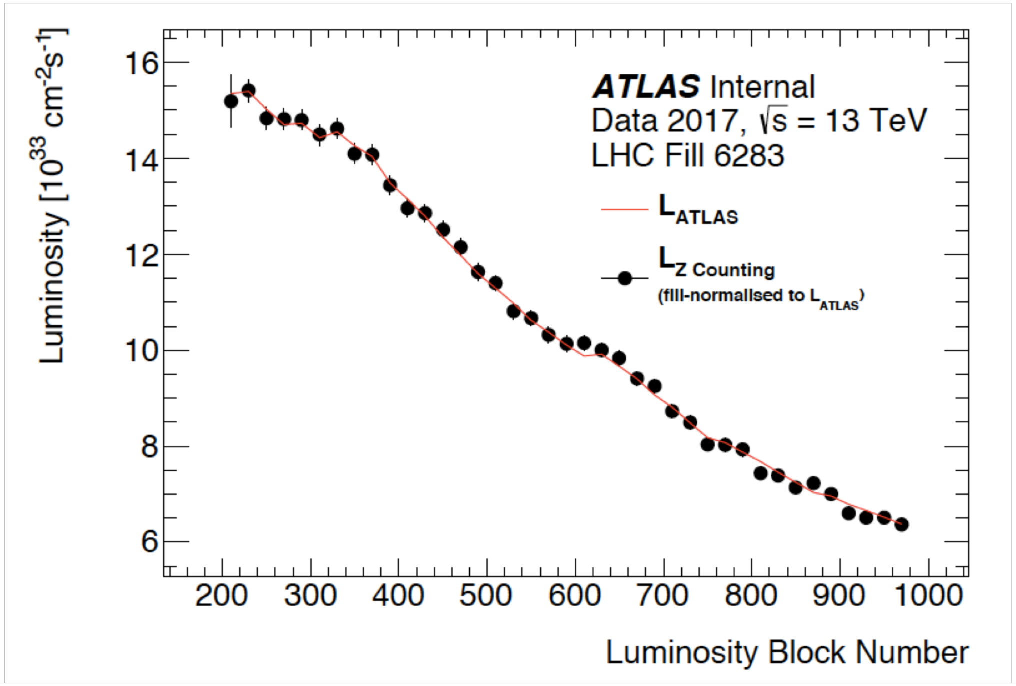

ATL-COM-DAPR-2018-011

Figure 2: *Top:* The instantaneous luminosity determined from the $Z \rightarrow \mu\mu$ counting rate, $L_{Z\,\mathrm{Counting}}$ (full circles), selecting two muons with $p_T^\mu > 27$ GeV, $|\eta^\mu| < 2.4$ and $66 < m_{\mu\mu} < 116$ GeV, and the ATLAS-preferred luminosity measurement L_{ATLAS} (red line) based on the LUCID online luminometer, both averaged over 20 Luminosity Blocks (LB). The LHC fill 6283 was taken at $\sqrt{s} = 13$ TeV on October 8, 2017. The Z counting rate is corrected for in situ data-driven trigger and reconstruction efficiencies including the residual Monte Carlo correction, and is normalised to the integrated ATLAS luminosity for this fill. The x-axis represents the elapsed time in units of Luminosity Blocks with a typical length of one minute per LB. Error bars are the statistical uncertainties of the $L_{Z\,\mathrm{Counting}}$ determination.

ATLAS Z-counting

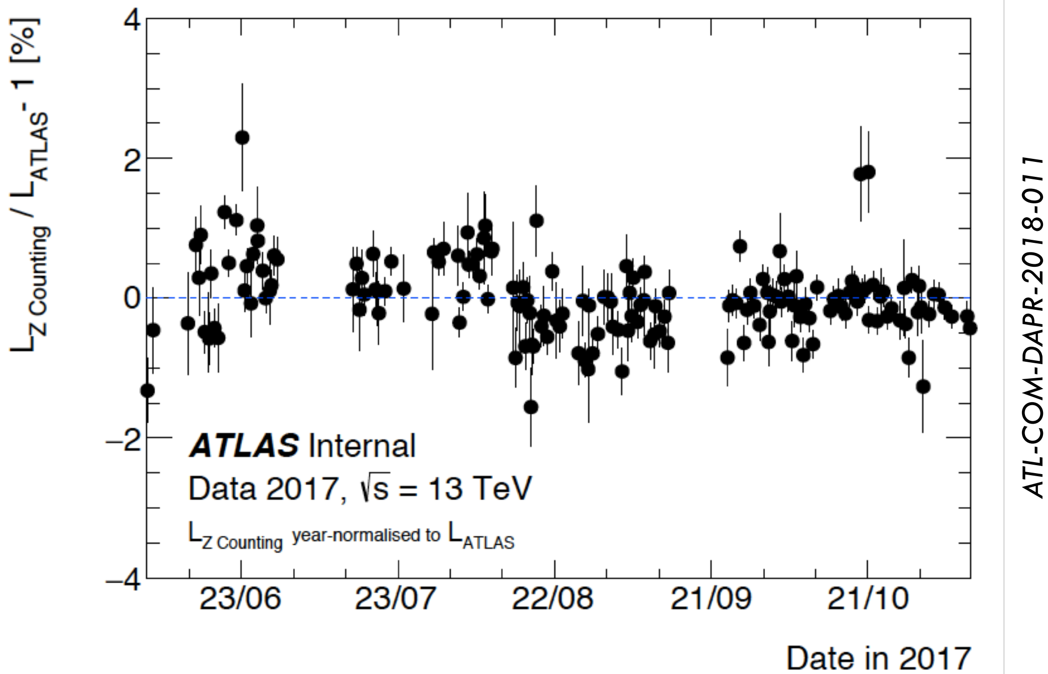

Figure 3: Fractional difference between the run-integrated luminosity determined from the $Z \to \mu\mu$ counting rate, $L_{Z\ Counting}$, selecting two muons with $p_T^\mu > 27$ GeV, $|\eta^\mu| < 2.4$ and $66 < m_{\mu\mu} < 116$ GeV, and the run-integrated, ATLAS-preferred luminosity measurement L_{ATLAS} (based on the LUCID online luminometer) per LHC fill taken at $\sqrt{s} = 13$ TeV in 2017. The Z counting rate is corrected for in situ data-driven trigger and reconstruction efficiencies including the residual Monte Carlo correction, and is normalised to the integrated ATLAS luminosity of the whole 2017 data taking period. The x-axis represents the date when the fill was recorded; only runs with at least 10,000 Z counts and a minimum length of about 40 min are included. Error bars reflect the statistical uncertainties of the $L_{Z\ Counting}$ measurements only. The dashed line indicates zero.

ATLAS/CMS Z-counting ratio

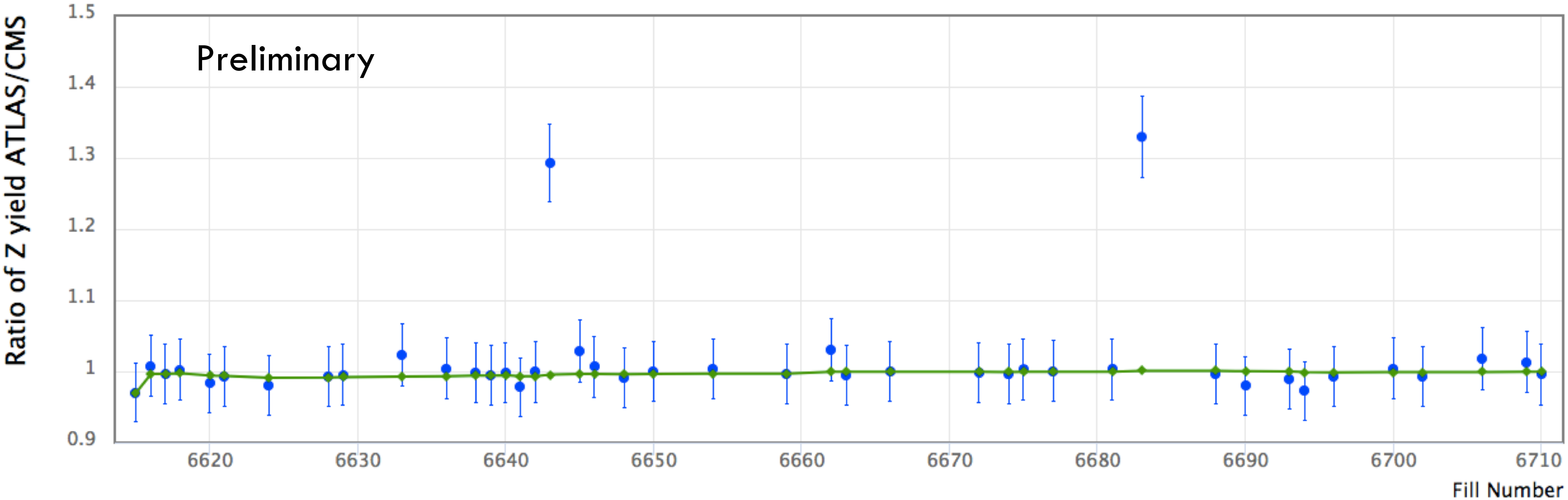

https://lpc.web.cern.ch/cgi-bin/plots.py

ATLAS: sistematica finale Run 2

- Integrated luminosity in each year L_i and its uncertainty σ_i
  - Covariance matrix of the absolute integrated luminosities in each year V_L
    - This encodes the correlations between the year-by-year luminosities
- Then $L_{\text{tot}} = \Sigma_i L_i$ and variance $\sigma^2_{L_{\text{tot}}} = \mathbf{G}\mathbf{V_L}\tilde{\mathbf{G}}$
  - Derivatives vector: $\mathbf{G} = \left(\frac{\mathrm{d}L_{\text{tot}}}{\mathrm{d}L_1}, \frac{\mathrm{d}L_{\text{tot}}}{\mathrm{d}L_2}, \frac{\mathrm{d}L_{\text{tot}}}{\mathrm{d}L_3}, \ldots\right) = (1, 1, 1, \ldots)$
  - Covariance matrix V_L constructed by summing individual sources with uncertainties σ_i in each year (many separate correlated/uncorrelated sources):

$$V_L = \underbrace{\begin{pmatrix} \sigma_1^2 & 0 & 0 \\ 0 & \sigma_2^2 & 0 \\ 0 & 0 & \sigma_3^2 \end{pmatrix}}_{\text{An uncorrelated source}} + \underbrace{\begin{pmatrix} \sigma_1^2 & \sigma_1\sigma_2 & \sigma_1\sigma_3 \\ \sigma_1\sigma_2 & \sigma_2^2 & \sigma_2\sigma_3 \\ \sigma_1\sigma_3 & \sigma_2\sigma_3 & \sigma_3^2 \end{pmatrix}}_{\text{A correlated source}} + \ldots$$

  - Some sources may not contribute to all years, so some σ_i=0
    - Sources with both correlated and uncorrelated parts are handled by being broken into two separate contributions to V_l

https://twiki.cern.ch/twiki/bin/view/Atlas/LuminosityForPhysics